Supporting Information

Application of 4-Pyridylselenolate Palladium Macrocycles in Suzuki Couplings

P. A. Mane,[a] A. K. Pathak,[a,b] N. Bhuvanesh[c] and S. Dey*[a,b]

[a] Chemistry Division, Bhabha Atomic Research Centre, Mumbai-400085, India.

[b] Homi Bhabha National Institute, Training School Complex, Mumbai-400094, India.

[c] Department of Chemistry, Texas A&M University, PO Box 30012, College Station, Texas 77842-3012, USA.

Email: dsandip@barc.gov.in (S. Dey); Tel: +91-22-2559-2589

Supporting Information

Table of Contents

General Procedures: Solvents were dried and distilled prior to use by standard methods. All reactions were carried out in Schlenk flasks under a nitrogen atmosphere. 4-Mercaptopyridine was used as purchased from commercial sources without further purification. $Pd(dppe)Cl_2$, $Pd(dppf)Cl_2$[1], $Pd(Xantphos)Cl_2$[2], $Pd(Xantphos)(OTf)_2$[3], $Pd(dppf)(OTf)_2$[4], $Pd(dppe)(OTf)_2$[5], $Pd(dppe)(4\text{-Sepy})_2$[6] and $4,4'\text{-py}_2Se_2$[7] were prepared according to literature method. Melting points were determined in capillary tubes and are uncorrected. Elemental analysis for C, H, N and S were carried out on an Carlo-Erba EA-1110 CHNS Analyser. ^{1}H NMR spectra were recorded on a Bruker and Varian NMR

spectrometers operating at 200.13, 300.13, 500.13, 600.13 and 800.13 MHz, chemical shifts are relative to internal acetone-d_6, dichloromethane-d_2 and chloroform-d_1 peak (δ 2.05, δ 5.32 and δ 7.26). The chemical shifts (δ) were reported in parts per million (ppm). The coupling constants (*J*) are quoted in Hertz (Hz). Proton splitting patterns are described as s (singlet), d (doublet), t (triplet), and m (multiplet). For $^{31}P\{^1H\}$ NMR spectra were recorded on a Bruker NMR spectrometer operating at 121.46 MHz, 243.17 MHz. $^{13}C\{^1H\}$ NMR spectra were recorded on a Bruker NMR spectrometer operating at 201.16 MHz. $^{19}F\{^1H\}$ NMR spectra were recorded on a Bruker NMR spectrometer operating at 282.38 MHz. Absorption spectra were recorded on a Jasco V–650 spectrophotometer. Mass spectra were recorded on a maXis Impact (Bruker) mass spectrometer.

Crystallography

The crystallographic data together with the data collection and refinement details are given in Table **S1** and **S2**. Crystals of **4**, **6a**, **7a**, **7b** and **9** were grown from solvent mixtures of acetone-hexane, acetonitrile-hexane, dichloromethane-hexane, acetone-hexane and dichloromethane-hexane at room temperature. Crystals of complex **10** was grown from solvent mixtures of acetone-hexane -5 ^oC. Single crystal X-ray diffraction data of complex **4** was collected on A BRUKER Venture X-ray diffractometer fitted with Cu Kα radiation at 100K. Single crystal X-ray diffraction data of complex **6a** was collected on A BRUKER APEX 3 diffractometer fitted with Mo Kα radition at 110K. Single crystal X-ray diffraction data of complex **7** was collected on A BRUKER Quest X-ray diffractometer fitted with Mo Kα radiation at 110K. The single crystal X-ray diffraction data of complex **7b** and complex **10** were collected on A BRUKER Quest X-ray diffractometer fitted with Cu Kα radiation at 110K. For **10**, although the formula is given as $C_{44}H_{36}NOP_2PdS{\cdot}1.47(CF_3O_3S){\cdot}C_3H_6O{\cdot}$[+MASKed solvent], for charge balance it could be written as $C_{44}H_{36}NOP_2PdS{\cdot}(CF_3O_3S){\cdot}0.47(CF_3O_3SH){\cdot}C_3H_6O{\cdot}$[+MASKed solvent].

We made no efforts to model partially occupied (0.47 H-atoms) disordered over different oxygen atoms in (CF_3O_3SH).

Single crystal X-ray diffraction data of complex **9** was collected on XtaLAB Synergy, Dualflex, HyPix four-circle diffractometer fitted with Cu Kα radiation at 100K. For above compounds the integrated intensity information for each reflection was obtained by reduction of the data frames with the program APEX3.[8] SADABS[9] was employed to correct the data for absorption effects. A solution was obtained readily using XT/XS in APEX3.[8,10-12] Hydrogen atoms were placed in idealized positions and were set riding on the respective parent atoms. All non-hydrogen atoms were refined with anisotropic thermal parameters. The structure was refined (weighted least squares refinement on F^2) to convergence.[10-13] Olex2 was employed for the final data presentation and structure plots.[13] SCALE3 ABSPACK[14,15] was employed to correct the data for absorption effects of complex **9**. The structure was refined (full-matrix least-squares methods against F^2) to convergence.[11-12] Final Cif was employed for the final data presentation and structure plots.[16]

Syntheses and spectroscopy of complexes

Pd(dppf)(4-Sepy)$_2$ (2)

An acetone solution of (10 mL) of $Pd(dppf)Cl_2$ (52.7 mg, 0.072 mmol) was added to a freshly prepared methanolic solution of (10 mL) of Na(4-Sepy) (prepared from 4,4′-py_2Se_2 (22.7 mg, 0.072 mmol) and $NaBH_4$ (5.5 mg, 0.145 mmol)) with stirring which continued for 4 h. The solvents were evaporated in vacuuo, the violet residue was washed with diethyl ether and extracted with dichloromethane (3 × 5 mL). A few drops of hexane were added to yield violet-colored crystals of **2** (60.8 mg, 0.062 mmol, 87%; mp 216 °C). Anal. Calcd for **2** $C_{44}H_{36}P_2PdSe_2FeN_2$: C, 54.21; H, 3.72; N, 2.87; Found: C, 53.85; H, 3.73; N, 3.30%. ^{1}H NMR (600 MHz, $CDCl_3$) δ: 4.18 (s, 4H, H$_\beta$-ferr), 4.36 (s, 4H, H$_\alpha$-ferr), 7.16 (d, $^3J_{H,H}$ = 5.0 Hz, 4H,

H$_\beta$-Py), 7.35 (t, $^3J_{H,H}$ = 7.5 Hz, 8H, *m*-H of Ph), 7.45 (t, $^3J_{H,H}$ = 7.5 Hz, 4H, *p*-H of Ph), 7.74-7.79 (m, 8H, *o*-H of Ph), 7.85 (d, $^3J_{H,H}$ = 5.0 Hz, 4H, H$_\alpha$-Py). $^{31}P\{^1H\}$ NMR (121 MHz, $CDCl_3$) δ: 21.3 (s, $^2J_{Se,P}$ = 52.2 Hz) ppm. $^{13}C\{^1H\}$ NMR ($CDCl_3$, 201 MHz) δ: 73.3 (s, *β*-C of ferr); 76.0 (s, *α*-C of ferr); 75.9 (d, $^1J_{P-C}$ = 50.3 Hz, i*pso*-C of ferr); 128.2 (s, *m*-C of Ph); 130.6 (s, *β*-C of Py); 131.2 (s, *p*-C of Ph); 132.1 (d, $^1J_{P-C}$ = 48.3 Hz, i*pso*-C of Ph); 134.7 (s, *o*-C of Ph); 146.9 (s, *α*-C of Py); 151.2 (s, i*pso*-C of Py).

Pd(Xantphos)(4-Sepy)$_2$ (3)

Prepared in similar manner to that for **2**, using Pd(Xantphos)Cl_2 (52.9 mg, 0.070 mmol) and Na(4-Sepy) (prepared from 4,4′-py$_2$Se$_2$ (22.0 mg, 0.070 mmol) and $NaBH_4$ (5.3 mg, 0.140 mmol)) and recrystallized from acetone-hexane mixture to yield brown powder of **3** (52.2 mg, 0.052 mmol, 75%; mp 148 °C) Anal. Calcd for **3** $C_{49}H_{40}N_2OP_2PdSe_2$: C, 58.90; H, 4.04; N, 2.80; Found: C, 58.14; H, 3.81; N, 2.59%. ^1H NMR (300 MHz, $CDCl_3$) δ: 1.75 (s, 6H, CH_3), 7.10-7.23 (m, 14H, H$_\beta$-Py + CHC*H*CH + *m*-H of Ph), 7.23-7.29 (m, 6H, *p*-H of Ph + CPC*H*CH), 7.37-7.50 (m, 8H, *o*-H of Ph), 7.57-7.63 (m, 2H, CHC*H*CC), 7.80 (d, $^3J_{H,H}$ = 5.1 Hz, 4H, H$_\alpha$-Py). $^{31}P\{^1H\}$ NMR (121 MHz, $CDCl_3$) δ: 10.6 (s) ppm.

[Pd$_3$(Xantphos)$_2$(4-Sepy)$_4$](OTf)$_2$ (4)

Prepared in similar manner to that for **6**, using Pd(Xantphos)(OTf)$_2$ (68.1 mg, 0.069 mmol) and **3** (69.2 mg, 0.069 mmol) and recrystallized from acetone-hexane mixture to yield red colored crystals of **4** (75.2 mg, 0.031 mmol, 45%; mp 184 °C). Anal. Calcd for **4** $C_{100}H_{80}F_6N_4O_8P_4Pd_3S_2Se_4$: C, 49.99; H, 3.36; N, 2.33; Found: C, 50.23; H, 3.52; N, 2.53%. ^1H NMR (300 MHz, $CDCl_3$) δ: 1.81 (s, CH_3), 6.85 (d, *J* = 6.0 Hz, H$_\beta$-Py), 6.90-6.98 (m, CH*CH*CH), 6.99-7.13 (m, *m*-H of Ph + CH*CH*CH), 7.14-7.29 (m, *p*-H of Ph + H$_\beta$-Py + CP*CH*CH), 7.30-7.52 (m, *o*-H of Ph + H$_\alpha$-py + CP*CH*CH), 7.56 (d, *J* = 6.0 Hz, CH*CH*CC). 7.63 (d, *J* = 6.0 Hz, H$_\alpha$-Py), 7.87 (d, *J* = 6.0 Hz, CH*CH*CC). $^{31}P\{^1H\}$ NMR (121 MHz, $CDCl_3$) δ: 22.8 (s) ppm.

[$Pd_2(dppf)_2(4\text{-}Sepy)_2$]$(BPh_4)_2$ (5)

A dichloromethane solution of (10 mL) of $Pd(dppf)Cl_2$ (41.1 mg, 0.056 mmol) was added to a methanolic solution of (10 mL) of Na(4-Sepy) (prepared from 4,4′-py_2Se_2 (8.8 mg, 0.028 mmol) and $NaBH_4$ (2.1 mg, 0.055 mmol)) with stirring which continued for 2 h. Then a methanolic solution of (5 mL) of $NaBPh_4$ (19.2 mg, 0.056 mmol) was added, the stirring was further continued for 4 h. The solvents were evaporated in vacuuo; the red residue was washed with diethyl ether and extracted with dichloromethane (3 × 5 mL). A few drops of hexane were added to yield red crystal of **5** (46.4 mg, 0.020 mmol, 73%; mp 180 °C). Anal. Calcd for **5** $C_{126}H_{104}P_4Pd_2Se_2Fe_2B_2N_2$: C, 66.55; H, 4.61; N, 1.23; Found: C, 65.98; H, 4.60; N, 1.21%. ^{1}H NMR (500 MHz, $CDCl_3$) δ: 3.87 (s, 4H, H$_\beta$-ferr), 4.34 (s, 4H, H$_\beta$-ferr), 4.62 (s, 4H, H$_\alpha$-ferr), 4.73 (s, 4H, H$_\alpha$-ferr), 6.59 (d, $^3J_{H,H}$ = 5.6 Hz, 4H, H$_\beta$-Py), 6.92 (t, $^3J_{H,H}$ = 7.1 Hz, 12H, *p*-H of BPh; the peak correspond to the 4H of H$_\alpha$-Py merged in the base), 7.08 (t, $^3J_{H,H}$ = 7.1 Hz, 24H, *m*-H of BPh; the peak correspond to the 8H of *m*-H of PPh merged in the base), 7.26-7.32 (m, 12H, *o*-H of PPh + *p*-H of PPh), 7.50 (br m, 16H, *o*-H of BPh), 7.53-7.56 (br t, $^3J_{H,H}$ = 7.3 Hz, 8H, *m*-H of PPh), 7.64 (t, $^3J_{H,H}$ = 7.3 Hz, 4H, *p*-H of PPh), 7.89 (dd, $^3J_{P,H}$ = 12.5 Hz, $^3J_{H,H}$ = 7.5 Hz, 8H, *o*-H of Ph). ^{31}P{^{1}H} NMR (243 MHz, $CDCl_3$) δ: 30.6 (s, P *trans* to Se), 34.2 (s, P *trans* to N) ppm.

[Pd(dppe)(4-Sepy)]$_n$$(OTf)_n$ (6: n = 2, **6a**; n = 4, **6b**)

A dichloromethane solution of (8 mL) of $Pd(dppe)(OTf)_2$ (59.1 mg, 0.074 mmol) was added to a dichoromethane solution of (8 mL) of $Pd(dppe)(4\text{-}Sepy)_2$ (**1**)[23] (60.1 mg, 0.073 mmol) with stirring which continued for 4 h. The solvent was evaporated in vacuuo; the yellow residue was washed with diethyl ether and extracted with acetonitrile (3 × 5 mL). A few drops of hexane were added to yield yellow crystals of **6** (112.8 mg, 0.070 mmol, 95%; mp > 230 °C). Anal. Calcd for **6** $C_{64}H_{56}F_6N_2O_6P_4Pd_2S_2Se_2$: C, 47.39; H, 3.48; N, 1.73; Found: C, 47.98; H, 3.46; N, 1.75%. UV/vis (acetonitrile): λ_{max} (ε in M^{-1} cm^{-1}) 305 (9651), 363 (8043), 384 (sh, 6638), 430

(1463) nm. ^{1}H NMR (600 MHz, CD_2Cl_2) δ: 2.45-2.58 (m, 4H, CH_2), 2.61-2.74 (m, 4H, CH_2), 7.18 (d, $^{3}J_{H,H}$ = 6.0 Hz, 4H, Hβ-Py, dimer), 7.38 (br m, 4H, Hα-Py), 7.47-7.55 (m, 16H, *m*-H of Ph + *o*-H of Ph), 7.58-7.63 (m, 4H, *p*-H of Ph), 7.67 (dt, $^{3}J_{H,H}$ = 7.5 Hz, $^{4}J_{P,H}$ = 2.5 Hz, 8H, *m*-H of Ph), 7.71 (t, $^{3}J_{H,H}$ = 7.5 Hz, 4H, *p*-H of Ph), 7.86 (dd, $^{3}J_{P,H}$ = 12.6 Hz, $^{3}J_{H,H}$ = 7.5 Hz, 8H, *o*-H of Ph). A peak at δ 7.03 (d, $^{3}J_{H,H}$ = 6.0 Hz, 4H, Hβ-Py) is assigned to the tetramer with the ratio 9:91 with the dimer. All other signals for dimer and tetramer are overlapped. $^{31}P\{^{1}H\}$ NMR (243 MHz, CD_2Cl_2) δ: dimer, 56.8 (s, P *trans* to Se), 62.7 (s, P *trans* to N); tetramer, 55.1 (s, P *trans* to Se), 61.0 (s, P *trans* to N) ppm, in 93:7 ratio. $^{13}C\{^{1}H\}$ NMR (CD_2Cl_2, 201 MHz) δ: 129.9 (d, $^{3}J_{C,P}$ = 10.1 Hz, *m*-C of Ph); 130.5 (d, $^{2}J_{C,P}$ = 12.1 Hz, *o*-C of Ph); 133.2 (d, $^{3}J_{C,P}$ = 10.1 Hz, *m*-C of Ph); 133.4 (s, *p*-C of Ph); 133.6 (s, *β*-C of Py); 133.8 (m, two i*pso*-C of Ph are merged); 134.3 (d, $^{2}J_{C,P}$ = 12.1 Hz, *o*-C of Ph); 137.2 (s, *p*-C of Ph); 149.5 (s, *α*-C of Py), 152.0 (s, i*pso*-C of Py); signals corresponding to PCH_2 group and triflate anion were not resolved probably due to its low intensity. ESI-MS (ion, relative intensity): *m/z* 1472.9 ([**6a** – OTf]$^{+}$, 52%), 1347.0 ([(**6a** + CH_3CN) – 2Sepy]$^{+}$, 30%), 1318.9 ([**6a** – ($2C_6H_5$ + OTf)]$^{+}$, 63%), 1218.0 ([(**6a** + $3CH_3CN$ + 2H) – ($3C_6H_5$ + 2OTf)]$^{+}$, 100%), 1188.9 ([(**6a** + Na) – (Sepy + 2OTf)]$^{+}$, 59%), 1088.1 ([(**6a** + $2CH_3CN$ + H) – (2Sepy + $2C_6H_5$ + OTf)]$^{+}$, 28%).

[Pd(dppf)(4-Sepy)]$_n$(OTf)$_n$ (7: n = 2, **7a**; n = 4, **7b**)

Prepared in similar manner to that for **6**, using Pd(dppf)$(OTf)_2$ (85.1 mg, 0.088 mmol) and **2** (86.5 mg, 0.088 mmol) and recrystallized from dichloromethane-hexane mixture to get red powder of **7** (152.7 mg, 0.079 mmol, 89%; mp > 230 °C). Anal. Calcd for **7** $C_{80}H_{64}F_6Fe_2N_2O_6P_4Pd_2S_2Se_2$: C, 49.69; H, 3.34; N, 1.45; Found: C, 48.95; H, 3.17; N, 1.40%. UV/vis (acetone): λ_{max} (ε in M^{-1} cm^{-1}) 328 (sh, 11336), 346 (13722), 368 (sh, 11887), 488 (2208) nm. ^{1}H NMR (CD_2Cl_2, 600 MHz) δ: dimer, 3.81; tetramer 3.85 (s, 4H, 85:15, Hβ-ferr), tetramer, 4.33; dimer, 4.34 (s, 4H, Hβ-ferr), tetramer, 4.66; dimer, 4.72 (s, 4H, 16:84, Hα-ferr); tetramer, 4.83; dimer, 4.93 (s, 4H, 15:85, Hα-ferr), tetramer, 6.86; dimer, 7.09 (d, $^{3}J_{H,H}$ = 6 Hz,

4H, H$_\beta$-Py), 7.22 (t, $^3J_{H,H}$ = 6 Hz, 8H, *m*-H of Ph), 7.37 (t, $^3J_{H,H}$ = 6 Hz, 4H, *p*-H of Ph), 7.49 (m, 16H, *o*-H of Ph + *m*-H of Ph), 7.69 (br s, 12H, *p*-H of Ph + H$_\alpha$-Py), tetramer, 7.79 (br s, 4H, H$_\alpha$-Py), 8.02 (m, 8H, *o*-H of Ph). $^{31}P\{^1H\}$ NMR (CD_2Cl_2, 243 MHz) δ: Tetramer, 25.2 (s), 28.9 (s); Dimer 27.6 (s), 29.6 (s) in 15:85 ratio. $^{13}C\{^1H\}$ NMR (CD_2Cl_2, 201 MHz) δ: 72.5 (d, $^1J_{P\text{-}C}$ = 54.3 Hz, i*pso*-C of ferr, D); 74.2 (d, $^2J_{P,C}$ = 8.0 Hz, *α*-C of ferr, D); 74.3 (d, $^2J_{P,C}$ = 8.0 Hz, *α*-C of ferr, T); 75.5, 75.6 (each d, $^2J_{P,C}$ = 8.0 Hz, *β*-C of ferr, T); 75.8 (d, $^3J_{P,C}$ = 8.0 Hz, *β*-C of ferr, D); 77.5 (d, $^2J_{P,C}$ = 10.1 Hz, *α*-C of ferr, T); 77.9 (d, $^2J_{P,C}$ = 10.1 Hz, *α*-C of ferr, D); 128.9 (s); 129.2 (d, $^3J_{P,C}$ = 10.1 Hz, *m*-C of Ph, D); 129.5 (d, $^2J_{P,C}$ = 10.1 Hz, *o*-C of Ph, D); 129.3 (s), 129.8 (d, *J* = 10.1 Hz), 130.2 (s), 130.5 (s), 130.6 (s) (*o*-/*m*-C of Ph, T; *ipso*-C of Ph, D and T); 131.9 (s, *p*-C of Ph, T); 132.3 (s, *p*-C of Ph, D); 132.6 (s, *β*-C of Py, T); 132.8 (s, *β*-C of Py, D); 133.9 (d, $^3J_{P,C}$ = 12.1 Hz, *m*-C of Ph, D), 134.4 (d, $^2J_{P,C}$ = 8.1 Hz, *o*-C of Ph, T); 135.4 (d, $^2J_{P,C}$ = 10.1 Hz, *o*-C of Ph, D); 137.3 (s, *p*-C of Ph, D); 148.9, 149.4 (each s, *α*-C of Py, D, T); 150.9 (s, *ipso*-C of Py, D).

ESI-MS (ion, relative intensity): *m/z* 2373.6 ([(**7b** + CH_3CN + H) – ($5C_6H_5$ + 4OTf + dppf)]$^+$, 1%), 2332.5 ([(**7b** + H) – ($5C_6H_5$ + 4OTf + dppf)]$^+$, 3%), 2182.5 ([(**7b** + $2CH_3CN$) – ($7C_6H_5$ + 4OTf + dppf + py)]$^+$, 5%), 1912.8 ([(Pd_3(dppf)$_3$(Sepy)$_2$ + 2H) – $5C_6H_5$]$^+$, 2%), 1791.7 ([(**7a** + $4CH_3CN$ + 2H) – $4C_6H_5$]$^+$, 95%), 1784.9 ([**7a** – OTf]$^+$, 100%), 1761.9 ([(Pd_2(dppf)$_2$(Sepy)$_2$Se + $3CH_3CN$ + H) – C_6H_5]$^+$, 53%), 1757.9 ([(Pd_2(dppf)$_2$(Sepy)$_2$Se + CH_3CN + H)]$^+$, 61%), 1731.7 ([(**7a** + $6CH_3CN$) – ($5C_6H_5$ + C_5H_4)]$^+$, 84%), 1557.9 ([**7a** – (py + 2OTf)]$^+$, 34%).

[Pd_2(dppf)$_2$(4-Sepy)$_2$](BF_4)$_2$ (8)

A dichloromethane solution of (10 mL) of Pd(dppf)Cl_2 (59.2 mg, 0.081 mmol) was added to a methanolic solution of (10 mL) of Na(4-Sepy) (prepared from 4,4′-py$_2$Se$_2$ (12.7 mg, 0.040 mmol) and $NaBH_4$ (3.1 mg, 0.082 mmol)) with stirring which continued for 4 h. Then an acetone solution of (5 mL) of $AgBF_4$ (16.0 mg, 0.081 mmol) was added, the stirring was further continued for overnight. Next day the solvents were evaporated in vacuuo; the red

residue was washed with diethyl ether and extracted with dichloromethane (3 × 5 mL). A few drops of diethyl ether were added to yield red solid of **8** (48.6 mg, 0.027 mmol, 66%; mp 156 °C). Anal. Calcd for **8** $C_{78}H_{64}B_2F_8P_4Pd_2Se_2Fe_2N_2$: C, 51.78; H, 3.57; N, 1.55; Found: C, 51.23; H, 3.73; N, 1.85%. ^{1}H NMR (300 MHz, $CDCl_3$) δ: 4.19 (br s, 8H, H$_\beta$-ferr), 4.41 (s, 8H, H$_\alpha$-ferr), 7.40 (br s, 16H, *m*-H of Ph), 7.49 (br s, 8H, *p*-H of Ph), 7.89 (br s, 16H, *o*-H of Ph), the peaks correspond to the 4H of H$_\beta$-py and H$_\alpha$-py each merged in the base. ^{31}P{^{1}H} NMR (121 MHz, $CDCl_3$) δ: 34.8 (s) ppm. ^{19}F{^{1}H} NMR (282 MHz, $CDCl_3$) δ: −152.07 (br, $^{10}BF^-$), −152.12 (br s, $^{11}BF^-$) ppm.

[Pd(dppe)(4-Spy)]$_2$(OTf)$_2$ (9)

A dichloromethane solution of (5 mL) of Pd(dppe)(OTf)$_2$ (54.3 mg, 0.067 mmol) was added to a freshly prepared methanolic solution of (5 mL) of 4-pySH (7.5 mg, 0.067 mmol) with stirring which continued for 4 h. The solvents were evaporated in vacuuo, the yellow residue was washed diethyl ether and extracted in acetone (3 × 5 mL). A few drops of hexane were added to get yellow powder which was recrystallized from dichloromethane-hexane mixture to yield yellow colored crystals of **9** (42.5 mg, 0.023 mmol, 68%; mp 146 °C). Anal. Calcd for **9**·$(CF_3SO_3H)_2$·$(H_2O)_2$, $C_{66}H_{62}F_{12}N_2O_{14}P_4Pd_2S_6$: C, 42.52; H, 3.35; N, 1.50; Found: C, 42.13; H, 2.89; N, 1.52%. ^{1}H NMR (300 MHz, $CDCl_3$) δ: 2.63 (d, $^2J_{P,H}$ = 22.9 Hz, 8H, CH_2), 7.36-7.76 (m, 48H, Ph + py). ^{31}P{^{1}H} NMR (121 MHz, $CDCl_3$) δ: 60.9 (s) ppm.

[Pd(Xantphos)(4-Spy)](OTf) (10)

Prepared in similar manner to that for **9**, using Pd(Xantphos)(OTf)$_2$ (162.3 mg, 0.165 mmol) and 4-pySH (18.3 mg, 0.165 mmol) and recrystallized from acetone-hexane mixture to yield red colored crystals of the title compound (159.6 mg, 0.146 mmol, 88%; mp 208 °C). Anal. Calcd for **10**·CF_3SO_3H, $C_{46}H_{37}F_6NO_7P_2PdS_3$: C, 50.49; H, 3.41; N, 1.28; Found: C, 50.37; H, 3.58; N, 1.27%. UV/vis (acetone): λ_{max} (ε in M^{-1} cm^{-1}) 328 (sh, 21495), 347 (27308), 424 (sh, 3474), 479 (2397) nm. ^{1}H NMR (600 MHz, acetone-*d*$_6$) δ: 1.87 (s, 6H, CH_3), 7.50 (t, $^3J_{H,H}$ =

7.5 Hz, 8H, *m*-H of Ph), 7.56-7.63 (m, 6H, *p*-H of Ph + H$_{\beta}$-py), 7.72-7.81 (m, 6H, H$_{\alpha}$-py + CHC*H*CH + CPC*H*CH), 7.84 (dd, $^{3}J_{P,H}$ = 13.1 Hz, $^{3}J_{H,H}$ = 6.3 Hz, 8H, *o*-H of Ph), 8.14 (d, 7.8 Hz, 2H, CHC*H*CC), $^{31}P\{^{1}H\}$ NMR (121 MHz, acetone-d_6): δ 25.9 (s) ppm. $^{13}C\{^{1}H\}$ NMR (acetone-d_6, 201 MHz) δ: 33.8 (s, CH_3); 35.4 (s, *C*CH_3); 127.5 (t, $^{3}J_{P,C}$ = 27.6 Hz, CP of $C_{15}H_{12}O$); 127.9 (s, CH of $C_{15}H_{12}O$); 128.5 (s, CH of $C_{15}H_{12}O$); 130.4 (s, *m*-C of Ph); 133.6 (s, *p*-C of Ph); 134.8 (s, *o*-C of Ph); 135.6 (s, *β*-C of Py); 137.5 (s, CH of $C_{15}H_{12}O$); 155.5 (s, *α*-C of Py); 171.7 (s, CO of $C_{15}H_{12}O$). The peaks correspond to *ipso*-C of Ph and C*C*C(CH_3) are merged with the other peaks.

Suzuki-Miyaura Cross-Coupling Reaction

An oven-dried flask was charged with aryl bromide (1.0 mmol), phenyl boronic acid (1.3 mmol), palladium complex **7** (0.1 mmol, equivalent to 0.2 mol % of Pd), DMA (3.0 mL), and aqueous K_2CO_3 (2 mmol, 1 mL) and was placed on an oil bath at 120 °C under a nitrogen atmosphere, and the reaction mixture was stirred until maximum conversion of aryl bromide to product occurred. The reaction mixture was cooled to room temperature, was diluted with water (10 mL), and neutralized by dropwise addition of dilute HCl (aq). The mixture was extracted with hexane (3 × 15 mL), washed with water (2 × 10 mL) followed by brine solution (2 × 10 mL) and dried over anhydrous Na_2SO_4. The solvent of the extract was removed with rotary evaporator, and the resulting residue was analyzed by ^{1}H NMR spectroscopy.

Density Functional Calculations

Full geometry optimizations are carried out for all the Pd complexes of dppe and dppf by employing BP86 density functional. The BP86 density functional is a generalized gradient approximation functional and is formed by the combination of Becke's 1988 exchange functional with Perdew's 1986 correlation functional.[17,18] Quasi Newton-Raphson based algorithm is used for geometry optimization. Gaussian type double split valence basis

functions, namely, 6-31G** are used for Se, N, P, C and H atoms and 3-21G* basis set for Pd and Fe atoms are used for the calculations. The solvent is modeled by using conductor like screening model (COSMO).[19] GAMESS suites of *ab initio* program systems on a LINUX cluster platform is employed to carry out all electronic structure calculations.[20] Molecular geometries and orbitals are visualized by using the MOLDEN and MOLEKEL program systems.[21,22]

References

1. T. Hayashi, M. Konishi, Y. Kobori, M. Kumada, T. Higuchi, K. Hirotsu, Dichloro [l,l/-bis(diphenylphosphino)ferrocene] palladium-(II): An Effective Catalyst for Cross-Coupling of Secondary and Primary Alkyl Grignard and Alkylzinc Reagents with Organic Halides, *J. Am. Chem. Soc.*, 1984, **106**, 158.
2. A. M. Johns, M. Utsunomiya, C. D. Incarvito, J. F. Hartwig, A Highly Active Palladium Catalyst for Intermolecular Hydroamination. Factors that Control Reactivity and Additions of Functionalized Anilines to Dienes and Vinylarenes, *J. Am. Chem. Soc.*, 2006, **128**, 1828.
3. P. A. Mane, S. Dey, A. K. Pathak, M. Kumar, N. Bhuvanesh, Xantphos-Capped Pd(II) and Pt(II) Macrocycles of Aryldithiolates: Structural Variation and Catalysis in C−C Coupling Reaction, *Inorg. Chem.*, 2019, **58**, 2965.
4. P. J. Stang, B. Olenyuk, J. Fan, A. M. Arif, Combining Ferrocenes and Molecular Squares: Self-Assembly of Heterobimetallic Macrocyclic Squares Incorporating Mixed Transition Metal Systems and a Main Group Element. Single-Crystal X-ray Structure of $[Pt(dppf)(H_2O)_2][OTf]_2$, *Organometallics*., 1996, **15**, 904.
5. S. Fallis, G. K. Anderson, N. P. Rath, Nucleophilic attack on or displacement of coordinated 1,5-cyclooctadiene. Structures of platinum complexes $[Pt\{\sigma:\eta^2\text{-}C_8H_{12}(PPh_3)\}(dppe)][ClO_4]_2$ and $[Pt(dppe)(H_2O)_2][O_3SCF_3]_2$, *Organometallics*., 1991, **10**, 3180.
6. K. V. Vivekananda, S. Dey, A. Wadawale, N. Bhuvanesh, V. K. Jain, Syntheses of Pd(II)/Pt(II) complexes with non-chelating 4-pyridylselenolate ligand ranging from mononuclear to macrocyclic structures and their utility as catalysts in Suzuki C–C coupling reaction, *Dalton Trans*., 2013, **42**, 14158.

7. B. Boduszek, R. Gancarz, Pyridine-4-Selenenyl Bromides as New Reagents for Seleenylation of Olefins, *J. prakt. Chem*., 1996, **338**, 186.
8. APEX3 "Program for Data Collection on Area Detectors" BRUKER AXS Inc., 5465 East Cheryl Parkway, Madison, WI 53711–5373 USA.
9. SADABS, G. M. Sheldrick, "Program for Absorption Correction of Area Detector Frames", BRUKER AXS Inc., 5465 East Cheryl Parkway, Madison, WI53711–5373 USA.
10. G. M. Sheldrick, SHELXT–Integrated space-group and crystal-structure determination, *ActaCryst*., 2015, **A71**, 3.
11. G. M. Sheldrick, Crystal structure refinement with SHELXL, *ActaCryst*., 2015, **C71**, 3.
12. G. M. Sheldrick, A short history of SHELX, *ActaCryst.*, 2008, **A64**, 112. XT, XS, BRUKER AXS Inc., 5465 East Cheryl Parkway, Madison, WI 53711–5373 USA.
13. O. V. Dolomanov, L. J. Bourhis, R. J. Gildea, J. A. K. Howard, H. Puschmann, OLEX2: A complete structure solution, refinement and analysis program, *J. Appl. Cryst.,* 2009, **42**, 339.
14. CrysAlisPro 1.171.40.57a (Rigaku Oxford Diffraction, 2019).
15. Empirical Absorption Correction Using Spherical Harmonics, Implemented in Scale3 Abspack Scaling Algorithm, Version 171.33.41, CrysAlisPro Oxford Diffraction Ltd. Yarnton, UK, 2009.
16. D. Kratzert, FinalCif, V61, https://www.xs3.uni-freiburg.de/research/finalcif.
17. A. D. Becke, Density-functional exchange-energy approximation with correct asymptotic behaviour, *Phys. Rev. A.,* 1988, **38**, 3098.
18. J. P. Perdew, Density-functional approximation for the correlation energy of the inhomogeneous electron gas, *Phys. Rev.* B., 1986, **33**, 8822.
19. P. Su, H. Li, Energy decomposition analysis of covalent bonds and intermolecular interactions, *J. Chem. Phys.*, 2009, **131**, 014102.
20. M. W. Schmidt, K. K. Baldridge, J. A. Boatz, S. T. Elbert, M. S. Gordon, J. H. Jensen, S. Koseki, N. Matsunaga, K. A. Nguyen, S. Su, T. L. Windus, M. Dupuis, J. A Montgomery, A. General atomic and molecular electronic structure system, *J. Comput. Chem*., 1993, **14**, 1347.
21. G. Schaftenaar, J. H. Noordik, Molden: a pre- and post-processing program for molecular and electronic structures. *J. Comp.-Aided Mol. Des.*, 2000, **14**, 123.
22. S. Portmann, H. Luthi, MOLEKEL: An Interactive Molecular Graphics Tool, *Chimia.,* 2000, **54**, 766.

Table S1 Crystallographic and structure refinement data for palladium complexes

Compound	**6a**	**7a**·CH_2Cl_2	**7b**
Chemical formula	$C_{64}H_{56}F_6N_2O_6P_4Pd_2S_2Se_2$	$C_{81}H_{66}Cl_2F_6Fe_2N_2O_6P_4Pd_2S_2Se_2$	$C_{160}H_{128}F_{12}Fe_4N_4O_{12}P_8Pd_4S_4Se_4$
Formula weight	1621.82	2018.67	3867.50
Crystal Size (mm^3)	0.307 x 0.081 x 0.076	0.204 x 0.165 x 0.072	0.127 x 0.032 x 0.024
Diffractometer	A BRUKER APEX 3	A BRUKER Quest X-ray	A BRUKER Venture X-ray
T/K	110	110	110
λ/Å	0.71073	0.71073	1.54178
Crystal system	Monoclinic	Monoclinic	Tetragonal
Space group	$P2_1/n$	$P2_1/c$	$P4/ncc$
a/Å	16.6522(5)	12.6538(10)	28.0952(5)
b/Å	10.2800(3)	16.2974(13)	28.0952(5)
c/Å	17.9838(5)	37.773(3)	22.2553(6)
α/°	90°	90°	90°
β/°	97.5510(10)	97.989(2)	90°
γ/°	90°	90°	90°
V/$Å^3$	3051.85(15)	7714.1(11)	17567.0(8)
ρ_{calc}, g cm^{-3}	1.765	1.738	1.462
Z	2	4	4
μ/mm^{-1}	2.029	2.048	8.436
Reflections collected	22708	241617	474756
Data/restraints/parameters	6966 / 0 / 397	17750 / 385 / 1043	7494 / 495 / 562
Final R1,*w*R2 indices	R1 = 0.0327 wR2 = 0.0638	R1 = 0.0371 wR2 = 0.0721	R1 = 0.0466 wR2 = 0.1036
R_1, wR_2 (all data)	R1 = 0.0497 wR2 = 0.0697	R1 = 0.0514 wR2 = 0.0804	R1 = 0.0586 wR2 = 0.1149
Largest diff.peak & hole [e$Å^{-3}$]	0.519 and -0.453	0.888 and -0.737	0.944 and -0.850

Table S2 Crystallographic and structure refinement data for palladium complexes

Compound	**4**	**9**·$(CF_3SO_3H)_2$·$(CHCl_3)_2$·H_2O	**10**·$(CF_3SO_3H)_{0.47}$·C_3H_6O
Chemical formula	$C_{100}H_{80}F_6N_4O_8P_4Pd_3S_2Se_4$	$C_{68}H_{61}Cl_6F_{12}N_2O_{13}P_4Pd_2S_6$	$C_{48.47}H_{42}F_{4.41}NO_{6.41}P_2PdS_{2.47}$
Formula weight	2402.72	2083.92	1072.35
Crystal Size (mm^3)	0.021 x 0.018 x 0.014	0.100 x 0.100 x 0.100	0.102 x 0.029 x 0.018
Diffractometer	A BRUKER Venture X-ray	XtaLAB Synergy, Dualflex, HyPix four-circle	A BRUKER Venture X-ray
T/K	100.0	100	110
λ/Å	1.54178	1.54178	1.54178
Crystal system	Triclinic	triclinic	Trigonal
Space group	*P*-1	*P*-1	*P*-3
a/Å	12.1772(4)	14.65160(10)	23.6600(11)
b/Å	14.4575(5)	16.68330(10)	23.6600(11)
c/Å	16.4829(5)	17.44540(10)	15.0947(7)
α/°	107.299(2)	105.9860(10)	90°
β/°	96.961(2)	90.7770(10)	90°
γ/°	113.037(2)	92.5240(10)	120°
V/$Å^3$	2454.67(15)	4093.95(5)	7317.9(8)
ρ_{calc}, g cm^{-3}	1.625	1.691	1.460
Z	1	2	6
μ/mm^{-1}	7.668	8.286	5.242
Reflections collected	43686	59419	43366
Data/restraints/parameters	7754 / 220 / 625	16864 / 412 / 1317	7145 / 143 / 636
Final R1,*w*R2 indices	R1 = 0.0796 wR2 = 0.1417	R_1 = 0.0725 wR_2 = 0.1893	R1 = 0.0981 wR2 = 0.2288
R_1, wR_2 (all data)	R1 = 0.1039 wR2 = 0.1565	R_1 = 0.0740 wR_2 = 0.1910	R1 = 0.1110 wR2 = 0.2357
Largest diff.peak & hole [e$Å^{-3}$]	1.514 and -0.930	5.58 and -2.29	2.750 and -1.044

Table S3 Selected interatomic distances [Å] and angles [°] of **4**

Pd1–Se1	2.5174(12)
Pd1–P1	2.339(3)
Pd1–P2	2.347(3)
Pd2–Se2	2.4346(10)
Pd1–Se2	2.4728(12)
Pd2–Se1	2.4300(10)
P1–Pd1–P2	102.55(9)
P1–Pd1–Se1	83.70(7)
P2–Pd1–Se1	157.74(7)
Se2–Pd1–Se1	79.75(4)
P1–Pd1–Se2	160.40(7)
Se2–Pd2–Se1	82.25(3)
Pd2–Se1–Pd1	84.18(3)
Pd2–Se2–Pd1	85.04(4)
Se2#–Pd2–Se1	97.75(3)

Table S4 Selected interatomic distances [Å] and angles [°] of **6a**, **7a**·CH_2Cl_2 and **7b** by X-ray diffraction analysis. The values in parenthesis were calculated applying BP86 DFT Functional.[a]

	6a	**7a**·CH_2Cl_2	**7b**
Pd1–Se1/Se1#	2.4773(3)	2.4525(4)	2.4780(6)
	(2.512)	(2.502)	(2.511)
Pd1–P1	2.2731(7)	2.3073(9)	2.3352(12)
	(2.315)	(2.351)	(2.372)
Pd1–P2	2.2518(8)	2.2659(8)	2.2761(13)
	(2.308)	(2.344)	(2.315)
Pd1–N1/N1#	2.121(2)	2.123(3)	2.107(4)
	(2.175)	(2.168)	(2.156)
Pd2–Se2	-	2.4941(4)	-
		(2.543)	
Pd2–N2	-	2.073(3)	-
		(2.168)	
P1–Pd1–P2	83.80(3)	101.64(3)	100.01(4)
	(84.71)	(99.00)	(99.55)
P1–Pd1–Se1/Se1#	171.57(2)	162.49(3)	173.04(4)
	(169.11)	(164.08)	(174.73)
P1–Pd1–N1/N1#	91.66(6)	89.32(7)	87.95(11)
	(93.70)	(88.51)	(88.73)
P2–Pd1–Se1/Se1#	91.17(6)	82.90(2)	85.52(3)
	(89.13)	(84.80)	(85.53)
P2–Pd1–N1/N1#	170.21(7)	164.38(8)	169.89(11)
	(173.49)	(167.34)	(168.61)
N1/N1#–Pd1–Se1#	94.31(6)	89.95(7)	86.12(10)
	(95.28)	(89.91)	(85.37)

[#] symmetry related atom. [a] Calculation was based on the cationic complex part.

Table S5 Selected interatomic distances [Å] and angles [°] of **10**·$(CF_3SO_3H)_{0.47}$·C_3H_6O

Pd1–S1	2.264(3)
Pd1–P1	2.272(3)
Pd1–P2	2.277(3)
Pd1–O1	2.118(6)
P1–Pd1–P2	169.66(10)
P1–Pd1–S1	94.14(10)
P2–Pd1–S1	95.54(10)

Table S6 Energy Parameters and Composition of Frontier Orbitals of Pd Complexes Calculated Applying BP86 DFT Functional[a].

	complex-6a		**complex-7a**		**complex-7b**	
Stability (kcal/mol)	-916		-1231		-1473	
HOMO-LUMO gap (eV)	1.76		1.43		1.52	
% composition of frontier orbitals	HOMO	LUMO	HOMO	LUMO	HOMO	LUMO
Fe	-	-	93	3	91	3
Pd	12	27	1	30	1	29
Se	76	9	1	11	1	10
P	2	24	2	24	2	25
N	2	9	1	9	1	9
C	7	30	1	22	3	23
H	1	1	1	1	1	1
Absorption peak (nm)	432 (430)[b]		496 (488)		-	
Oscillator strength	0.07		0.08		-	
			Bond order			
Pd–Se	0.36		0.55		0.52	
Pd–N	0.50		0.35		0.35	
Pd–P	0.30		0.33		0.40	

[a] Calculation was based on the cationic complex part.

[b] Experimental values are shown in the parentheses.

Table S7 Calculated and experimental peaks of the fragmented ions of **[Pd(dppe)(4-Sepy)]$_n$(OTf)$_n$(6: n = 2, 6a; n = 4, 6b)**.

m/z	Ion	Calculated peak of the most abundant ion	Experimental peak of the most abundant ion
1627.9	$[(6a + 2CH_3CN + H) – C_6H_5]^+$ $(C_{62}H_{58}F_6N_4O_6P_4Pd_2S_2Se_2)^+$	1628.93	1628.89
1472.9	$[6a – OTf]^+$ $(C_{63}H_{56}F_3N_2O_3P_4Pd_2SSe_2)^+$	1472.95	1472.93
1347.0	$[(6a + CH_3CN) – 2Sepy]^+$ $(C_{56}H_{51}F_6NO_6P_4Pd_2S_2)^+$	1350.02	1350.01
1318.9	$[6a – (2C_6H_5 + OTf)]^+$ $(C_{51}H_{46}F_3N_2O_3P_4Pd_2SSe_2)^+$	1318.87	1318.93
1289.9	$[(6a + CH_3CN + 2H) – (2C_6H_5 + 2OTf)]^+$ $(C_{58}H_{56}N_3P_4Pd_2Se_2)^+$	1290.00	1289.88
1218.0	$[(6a + 3CH_3CN + 2H) – (3C_6H_5 + 2OTf)]^+$ $(C_{50}H_{52}N_5P_4Pd_2Se_2)^+$	1217.97	1218.03
1188.9	$[(6a + Na) – (Sepy + 2OTf)]^+$ $(C_{57}H_{52}NNaP_4Pd_2Se)^+$	1189.03	1188.98
1088.1	$[(6a + 2CH_3CN + H) – (2Sepy + 2C_6H_5 + OTf)]^+$ $(C_{45}H_{45}N_2P_4Pd_2SF_3O_3)^+$	1088.02	1088.09

Table S8 Calculated and experimental peaks of the fragmented ions of **[Pd(dppf)(4-Sepy)]$_n$(OTf)$_n$ (7: n = 2, 7a; n = 4, 7b)**

m/z	Ion	Calculated peak of the most abundant ion	Experimental peak of the most abundant ion
2373.6	$[(\mathbf{7b} + CH_3CN + H) - (5C_6H_5 + 4OTf + dppf)]^+$ $(C_{94}H_{79}Fe_3N_5P_6Pd_4Se_4)^+$	2373.61	2373.64
2332.5	$[(\mathbf{7b} + H) - (5C_6H_5 + 4OTf + dppf)]^+$ $(C_{92}H_{76}Fe_3N_4P_6Pd_4Se_4)^+$	2332.58	2332.58
2182.5	$[(\mathbf{7b} + 2CH_3CN) - (7C_6H_5 + 4OTf + dppf + py)]^+$ $(C_{79}H_{67}Fe_3N_5P_6Pd_4Se_4)^+$	2181.52	2181.62
1912.8	$[(Pd_3(dppf)_3(Sepy)_2 + 2H) - 5C_6H_5]^+$ $(C_{82}H_{69}Fe_3N_2P_6Pd_3Se_2)^+$	1912.77	1912.77
1791.7	$[(\mathbf{7a} + 4CH_3CN + 2H) - 4C_6H_5]^+$ $(C_{64}H_{58}F_6Fe_2N_6P_4Pd_2Se_2O_6S_2)^+$	1791.81	1791.68
1784.9	$[\mathbf{7a} - OTf]^+$ $(C_{79}H_{64}F_3Fe_2N_2O_3P_4Pd_2SSe_2)^+$	1784.89	1784.86
1761.9	$[(Pd_2(dppf)_2(Sepy)_2Se + 3CH_3CN + H) - C_6H_5]^+$ $(C_{78}H_{69}Fe_2N_5P_4Pd_2Se_3)^+$	1760.91	1760.82
1757.9	$[(Pd_2(dppf)_2(Sepy)_2Se + CH_3CN + H)]^+$ $(C_{80}H_{68}Fe_2N_3P_4Pd_2Se_3)^+$	1755.89	1755.82
1731.7	$[(\mathbf{7a} + 6CH_3CN) - (5C_6H_5 + C_5H_4)]^+$ $(C_{57}H_{53}F_6Fe_2N_8O_6P_4Pd_2S_2Se_2)^+$	1731.78	1731.77
1641.9	$[(\mathbf{7a} + 2CH_3CN + H) - (C_6H_5 + 2OTf)]^+$ $(C_{76}H_{66}Fe_2N_4P_4Pd_2Se_2)^+$	1641.96	1641.93
1630.8	$[\mathbf{7a} - (2C_6H_5 + OTf)]^+$ $(C_{67}H_{54}F_3Fe_2N_2O_3P_4Pd_2SSe_2)^+$	1630.81	1630.86
1601.9	$[(\mathbf{7a} + CH_3CN + 2H) - (C_6H_5 + 2OTf)]^+$ $(C_{74}H_{64}Fe_2N_3P_4Pd_2Se_2)^+$	1601.94	1601.82
1557.9	$[\mathbf{7a} - (py + 2OTf)]^+$ $(C_{73}H_{60}Fe_2NP_4Pd_2Se_2)^+$	1557.90	1557.87
817.9	$[Pd(dppf)(Sepy)]^+$ $(C_{39}H_{32}FeNP_2PdSe)^+$	817.97	817.96

Table S9 Optimization of reaction parameters of reaction between 4-bromoacetophenone and phenyl boronic acid[a]

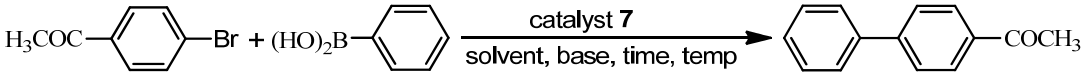

entry	solvent	base	temp (˚C)	time (h)	% yield[b]
Effect of Solvent					
1	Methanol	K_2CO_3	120	6	24
2	DMA	K_2CO_3	120	6	71
3	DMF	K_2CO_3	120	6	46
4	Dioxane	K_2CO_3	120	6	16
5	Acetone	K_2CO_3	120	6	12
Effect of Base					
6	DMA	K_2CO_3	120	6	71
7	DMA	Cs_2CO_3	120	6	13
8	DMA	KOH	120	6	15
9	DMA	Bu_4NOH	120	6	25
10	DMA	NaOAc	120	6	5
Effect of Temperature					
11	DMA	K_2CO_3	80	6	16
12	DMA	K_2CO_3	100	6	41
13	DMA	K_2CO_3	110	6	60
14	DMA	K_2CO_3	120	6	71

[a]Reaction conditions: Aryl bromide (1.0 mmol), phenyl boronic acid (1.3 mmol), base (2 mmol) in H_2O, DMA (3 mL), 0.2 mol% of Pd added, [b]Determined by ^1H NMR spectroscopy. $[Pd(dppf)(4\text{-}C_5H_4NSe)]_n(OTf)_n$ (**7**).

Table S10 Variation of time of reaction of 4-bromoacetophenone and phenyl boronic acid[a]

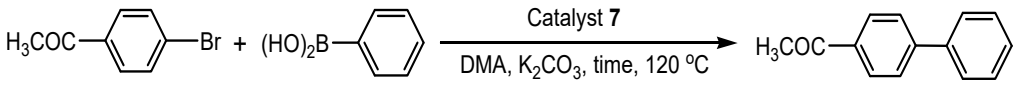

entry	Time (hrs)	mol% of Pd	yield (%)[b]	TON
1	0.5	0.2	8	40
2	1	0.2	16	80
3	2	0.2	29	145
4	4	0.2	51	255
5	6	0.2	72	360
6	8	0.2	87	435
7	9	0.2	94	470
8	10	0.2	100	500

[a]Reaction conditions: Aryl bromide (1.0 mmol), phenyl boronic acid (1.3 mmol), K_2CO_3 (2 mmol) in H_2O, DMA (3 mL). [b]Determined by ^1H NMR spectroscopy.

Table S11 Reaction between aryl halide and phenyl boronic acid by Pd complexes of 4-pyridylselenolate ligand.[a]

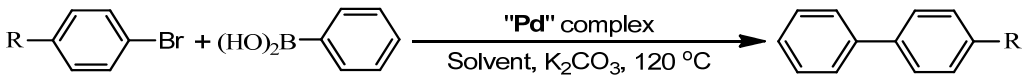

Entry	Ar–X	Complex	Solvent	Temp (°C)	mol% of "Pd"	Time (h)	% yield[b]	TON
1	4-$CH_3C_6H_4Br$	***trans*-[PdCl(4-SeC_5H_4N)(PPh_3)$_2$]**	1,4-dioxane	100	0.1	20	39[c]	390
2	4-$CH_3C_6H_4Br$	***trans*-[PdCl(4-SeC_5H_4N)(PPh_3)$_2$]**	1,4-dioxane	100	0.3	8	40[c]	133
3	4-$CH_3C_6H_4Br$	***trans*-[PdCl(4-SeC_5H_4N)(PPh_3)$_2$]**	1,4-dioxane	100	0.5	8	80[c]	166
4	4-$CH_3C_6H_4Br$	**7**	DMA	120	0.2	10	91	455
5	4-$CH_3COC_6H_4Br$	***trans*-[PdCl(4-SeC_5H_4N)(PPh_3)$_2$]**	1,4-dioxane	100	0.01	12	14[c]	1400
6	4-$CH_3COC_6H_4Br$	**[PdCl(4-SeC_5H_4N)(PPh_3)]$_n$**	1,4-dioxane	100	0.01	12	29[c]	2900
7	4-$CH_3COC_6H_4Br$	**7**	DMA	120	0.01	10	92	9200

[a]Reaction conditions: Aryl bromide (1.0 mmol), phenyl boronic acid (1.3 mmol), base (2 mmol) in H_2O, solvent (3 mL), mol% of Pd added. [b]Determined by ^1H NMR spectroscopy. [c]Vivekananda *et al*.[6]

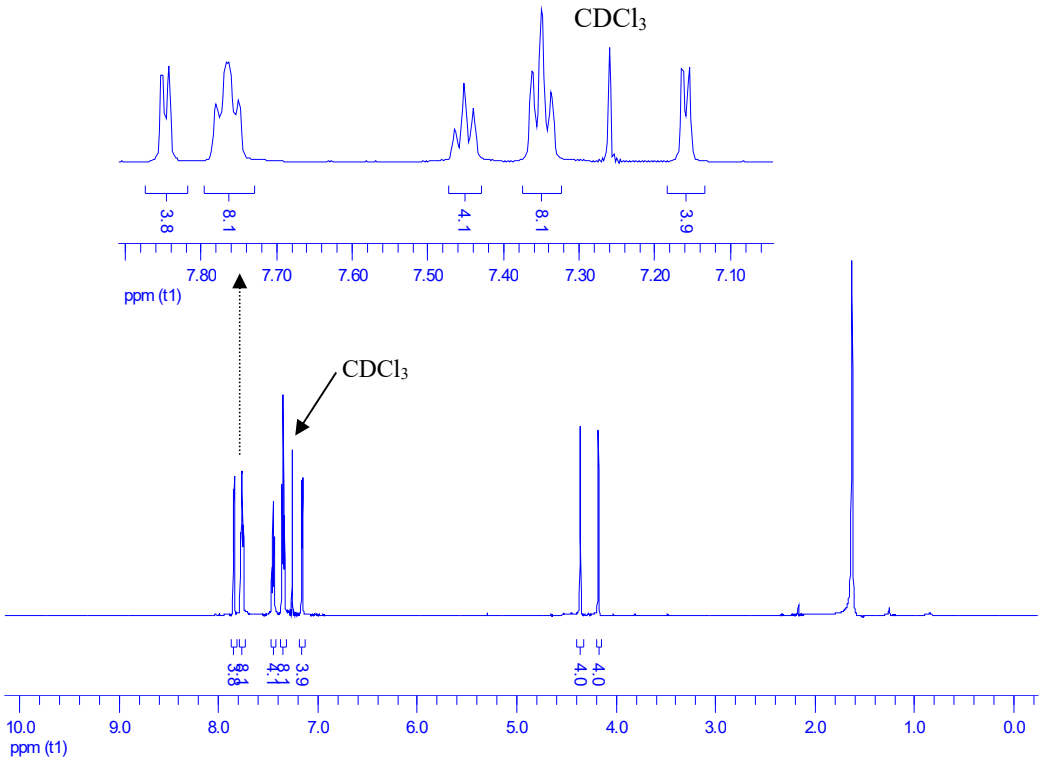

Fig. S1 ^{1}H NMR (600 MHz, $CDCl_3$, 298 K) spectra of **2**. δ: 4.18 (s, 4H, H$_\beta$-ferr), 4.36 (s, 4H, H$_\alpha$-ferr), 7.16 (d, $^{3}J_{H,H}$ = 5.0 Hz, 4H, H$_\beta$-Py), 7.35 (t, $^{3}J_{H,H}$ = 7.5 Hz, 8H, *m*-H of Ph), 7.45 (t, $^{3}J_{H,H}$ = 7.5 Hz, 4H, *p*-H of Ph), 7.74-7.79 (m, 8H, *o*-H of Ph), 7.85 (d, $^{3}J_{H,H}$ = 5.0 Hz, 4H, H$_\alpha$-Py).

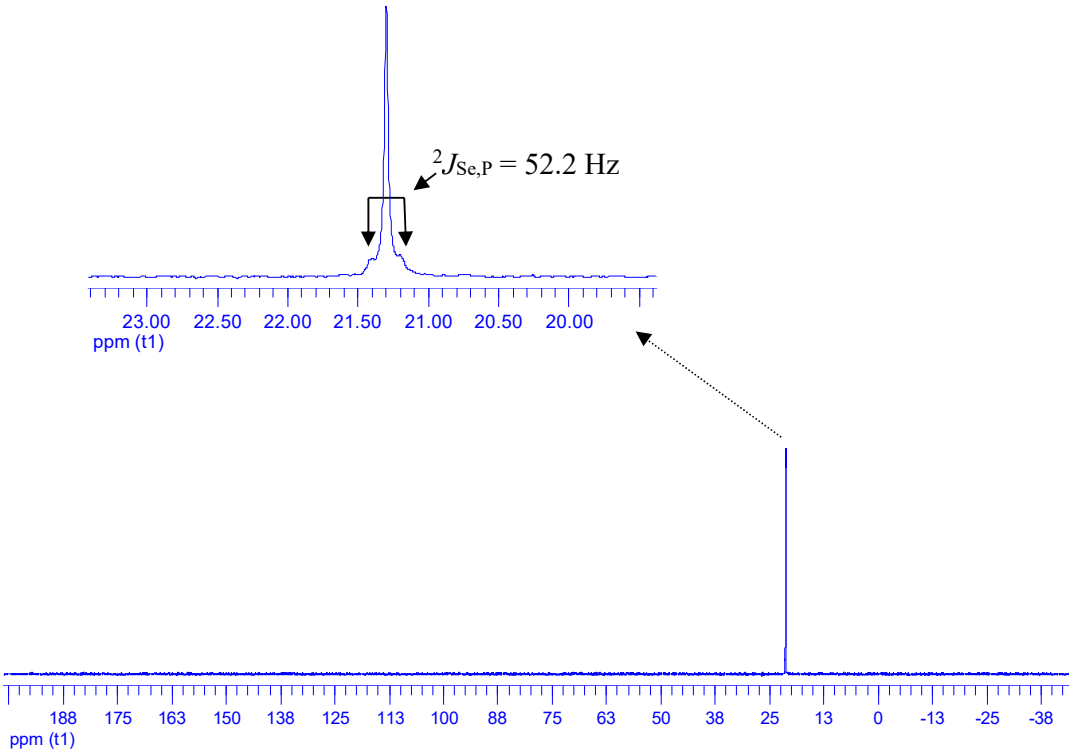

Fig. S2 $^{31}P\{^1H\}$ NMR (121 MHz, $CDCl_3$, 298 K) spectra of **2**. δ: 21.3 (s, $^2J_{Se,P}$ = 52.2 Hz) ppm.

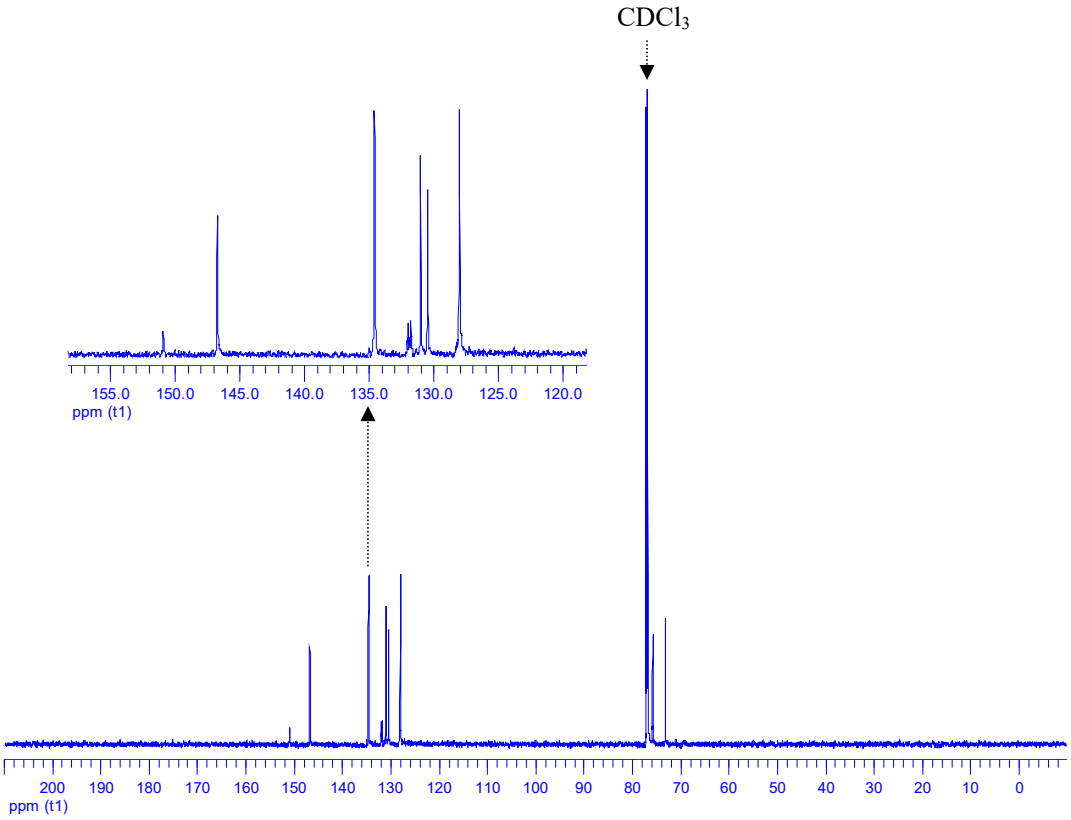

Fig. S3. $^{13}C\{^{1}H\}$ NMR (201 MHz, $CDCl_3$, 298 K) spectra of **2**. δ: 73.3 (s, *β*-C of ferr); 76.0 (s, *α*-C of ferr); 75.9 (d, $^{1}J_{P\text{-}C}$ = 50.3 Hz, i*pso*-C of ferr); 128.2 (s, *m*-C of Ph); 130.6 (s, *β*-C of Py); 131.2 (s, *p*-C of Ph); 132.1 (d, $^{1}J_{P\text{-}C}$ = 48.3 Hz, i*pso*-C of Ph); 134.7 (s, *o*-C of Ph); 146.9 (s, *α*-C of Py); 151.2 (s, i*pso*-C of Py).

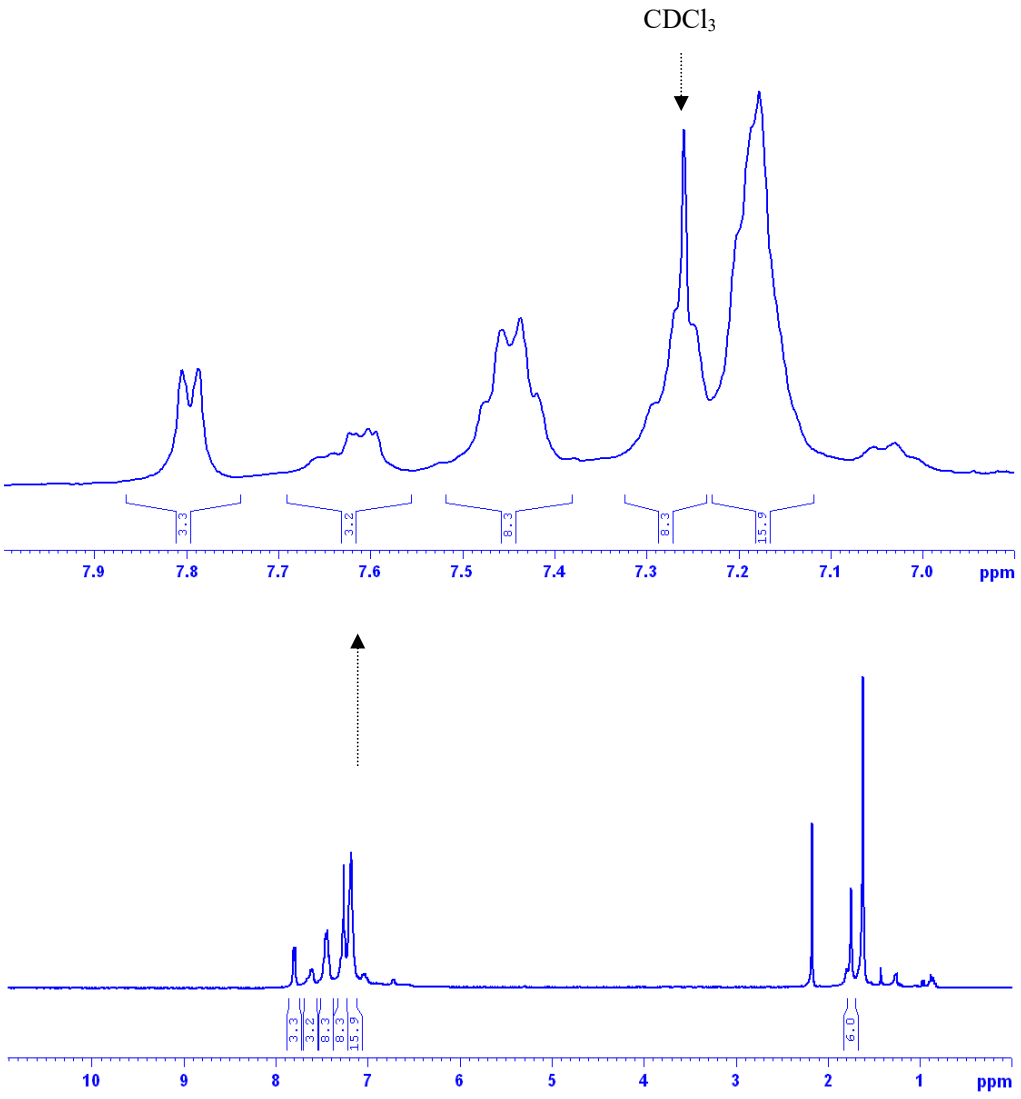

Fig. S4 ^{1}H NMR (300 MHz, $CDCl_3$, 298 K) spectra of **3**. δ: 1.75 (s, 6H, CH_3), 7.10-7.23 (m, 14H, H$_\beta$-Py + CHC*H*CH + *m*-H of Ph), 7.23-7.29 (m, 6H, *p*-H of Ph + CPC*H*CH), 7.37-7.50 (m, 8H, *o*-H of Ph), 7.57-7.63 (m, 2H, CHC*H*CC), 7.80 (d, $^{3}J_{H,H}$ = 5.1 Hz, 4H, H$_\alpha$-Py).

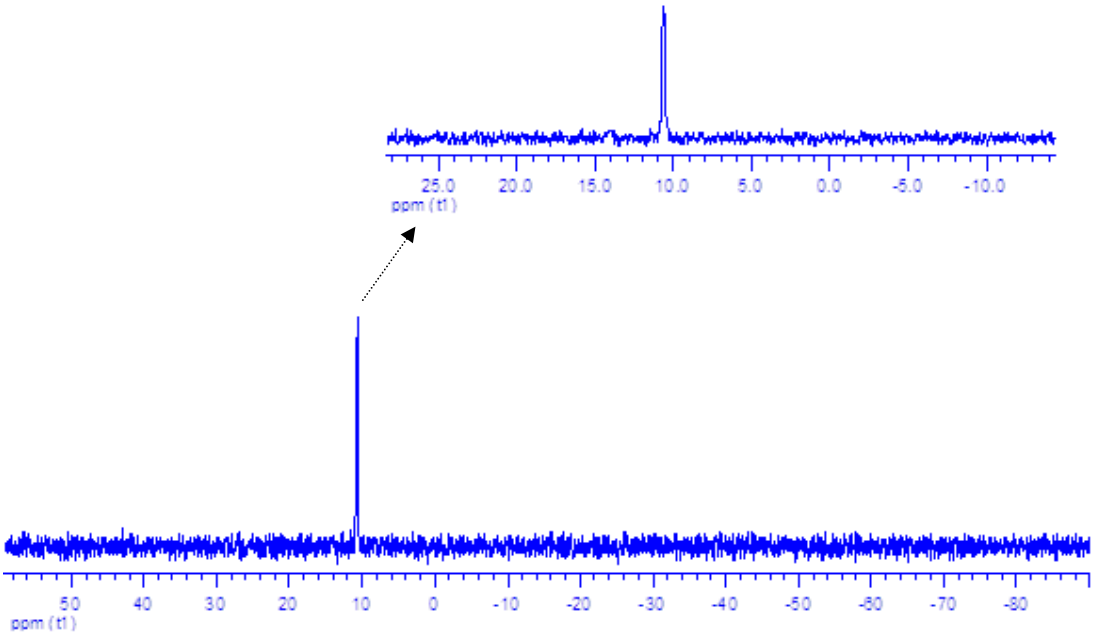

Fig. S5 $^{31}P\{^{1}H\}$ NMR (121 MHz, $CDCl_3$, 298 K) spectra of **3**. δ: 10.6 (s) ppm.

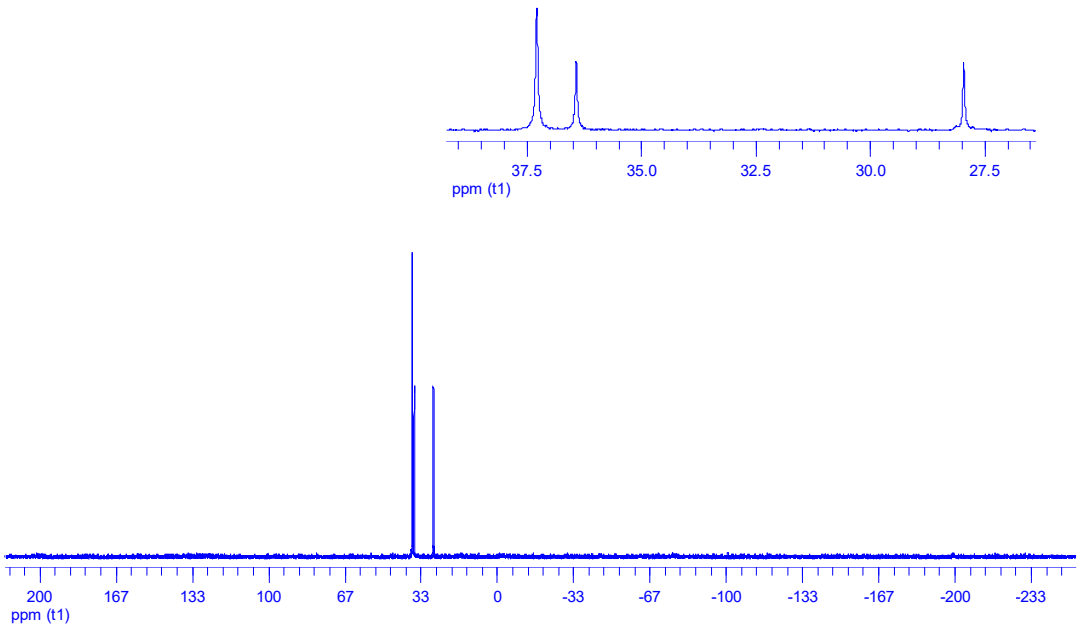

Fig. S6 $^{31}P\{^{1}H\}$ NMR (243 MHz, $CDCl_3$, 298 K) spectra of the reaction of $Pd(dppf)(OTf)_2$ and Na(4-Sepy) in 1:1 ratio.

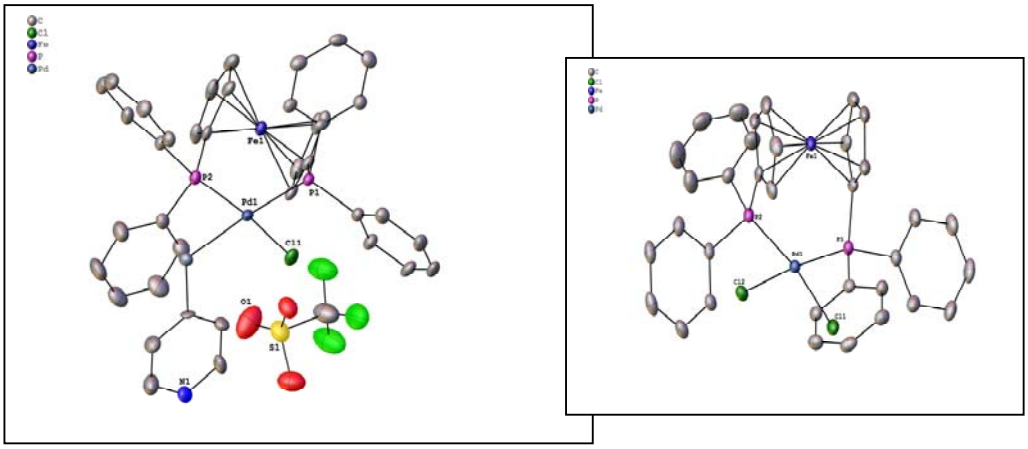

Fig. S7 ORTEP diagram of complexes Pd(dppf)Cl(4-Sepy) and Pd(dppf)Cl_2 in the crystal obtained from the reaction of Pd(dppf)$(OTf)_2$ and Na(4-Sepy). The hydrogen atoms are omitted for clarity.

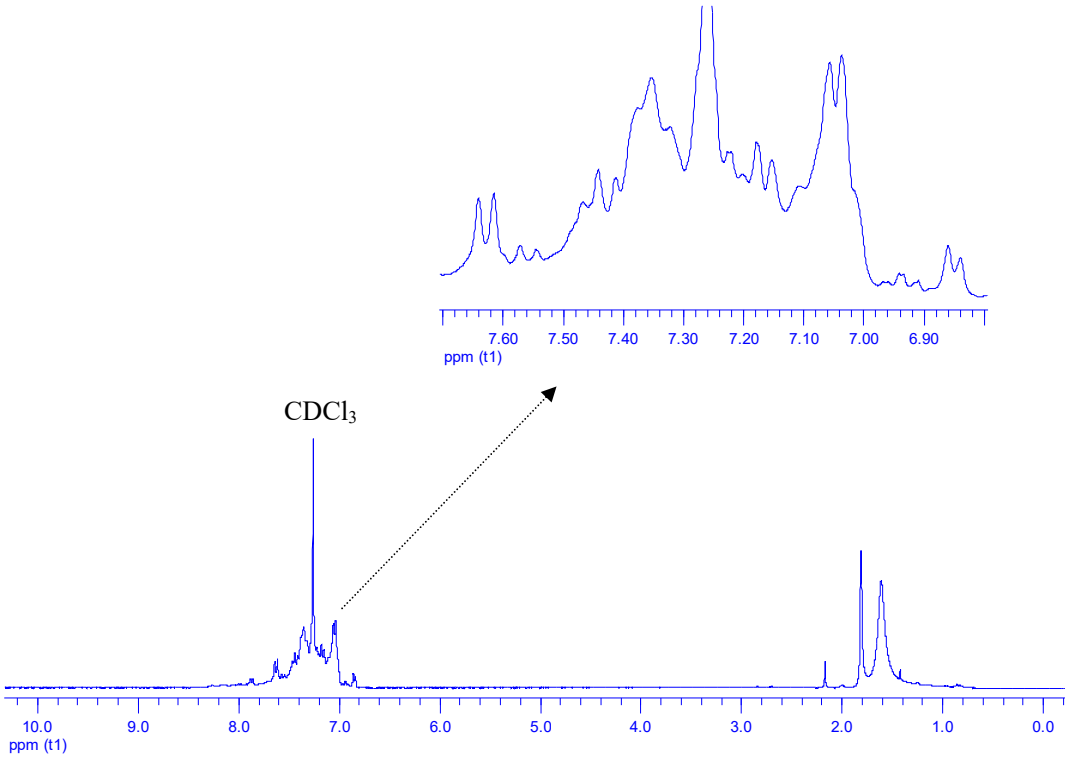

Fig. S8 ^{1}H NMR (300 MHz, $CDCl_3$, 298 K) spectra of **4**. δ: 1.81 (s, CH_3), 6.85 (d, J = 6.0 Hz, H$_\beta$-Py), 6.90-6.98 (m, CH*CH*CH), 6.99-7.13 (m, *m*-H of Ph + CH*CH*CH), 7.14-7.29 (m, *p*-H of Ph + H$_\beta$-Py + CP*CH*CH), 7.30-7.52 (m, *o*-H of Ph + H$_\alpha$-py + CP*CH*CH), 7.56 (d, J = 6.0 Hz, CH*CH*CC). 7.63 (d, J = 6.0 Hz, H$_\alpha$-Py), 7.87 (d, J = 6.0 Hz, CH*CH*CC).

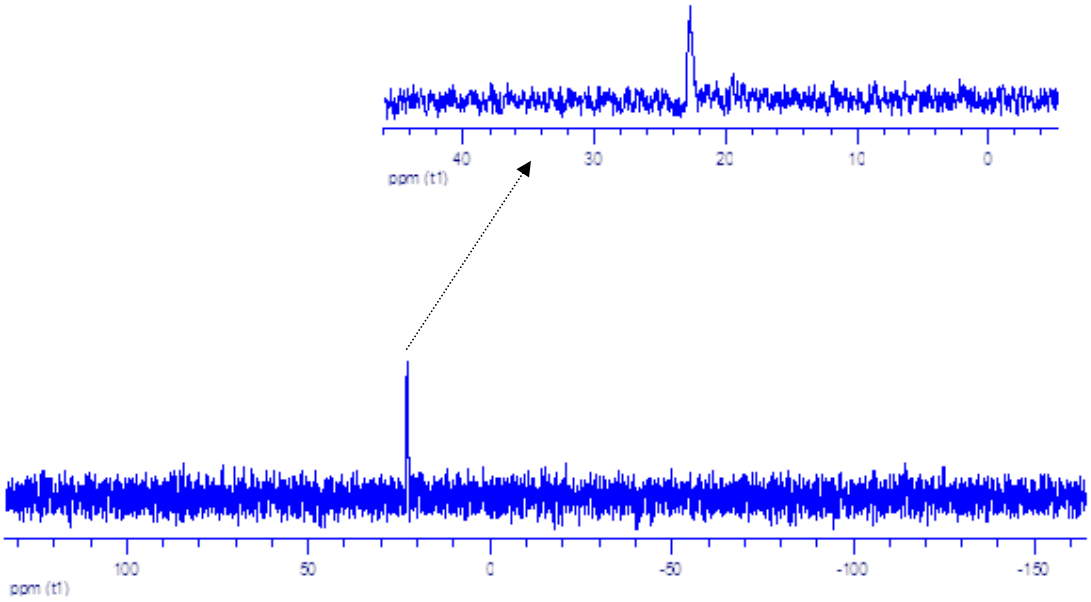

Fig. S9 $^{31}P\{^{1}H\}$ NMR (121 MHz, $CDCl_3$, 298 K) spectra of **4**. δ: 22.8 (s) ppm.

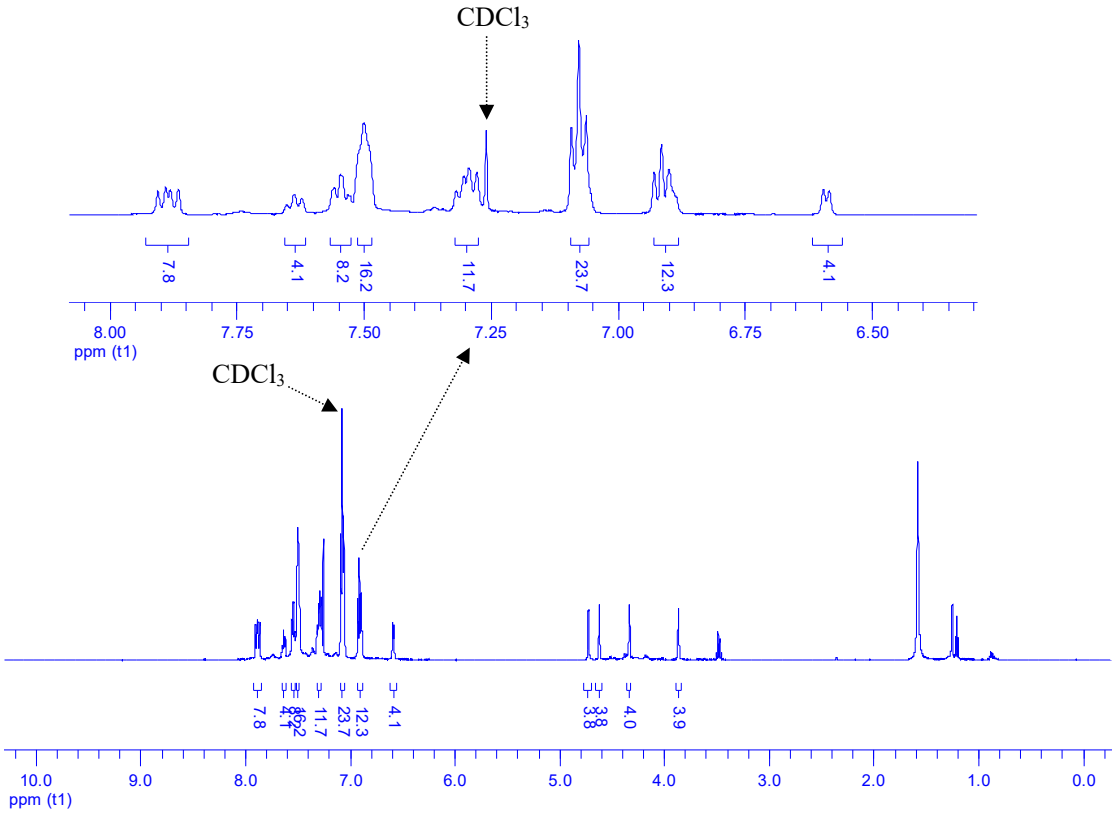

Fig. S10 ^{1}H NMR (500 MHz, $CDCl_3$, 298 K) spectra of **5**. δ: 3.87 (s, 4H, H$_\beta$-ferr), 4.34 (s, 4H, H$_\beta$-ferr), 4.62 (s, 4H, H$_\alpha$-ferr), 4.73 (s, 4H, H$_\alpha$-ferr), 6.59 (d, $^{3}J_{H,H}$ = 5.6 Hz, 4H, H$_\beta$-Py), 6.92 (t, $^{3}J_{H,H}$ = 7.1 Hz, 12H, *p*-H of BPh; the peak correspond to the 4H of H$_\alpha$-Py merged in the base), 7.08 (t, $^{3}J_{H,H}$ = 7.1 Hz, 24H, *m*-H of BPh; the peak correspond to the 8H of *m*-H of PPh merged in the base), 7.26-7.32 (m, 12H, *o*-H of PPh + *p*-H of PPh), 7.50 (br m, 16H, *o*-H of BPh), 7.53-7.56 (br t, $^{3}J_{H,H}$ = 7.3 Hz, 8H, *m*-H of PPh), 7.64 (t, $^{3}J_{H,H}$ = 7.3 Hz, 4H, *p*-H of PPh), 7.89 (dd, $^{3}J_{P,H}$ = 12.5 Hz, $^{3}J_{H,H}$ = 7.5 Hz, 8H, *o*-H of Ph).

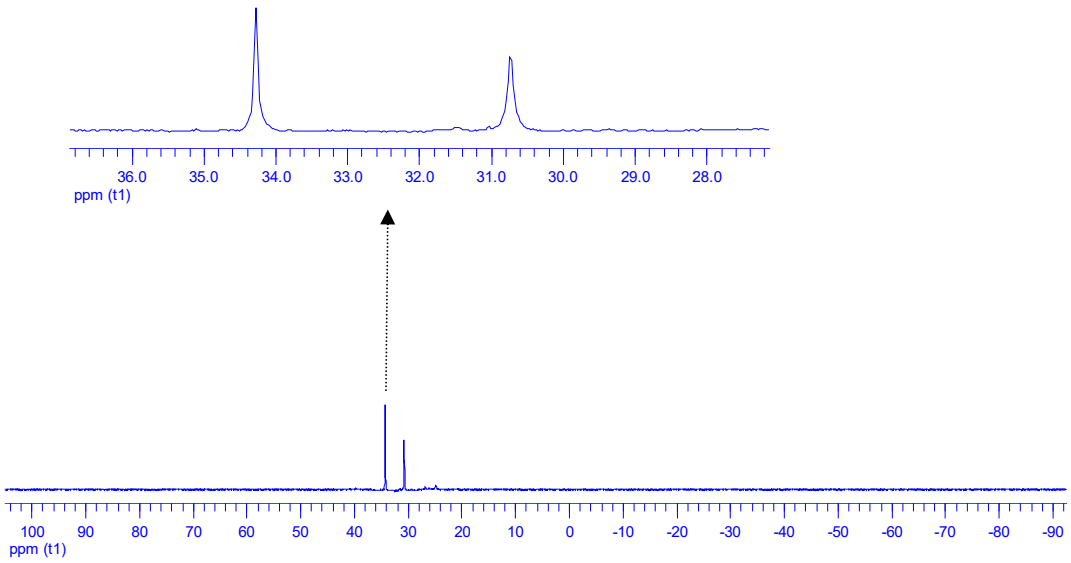

Fig. S11 $^{31}P\{^{1}H\}$ NMR (243 MHz, $CDCl_3$, 298 K) spectra of **5**. δ: 30.6 (s, P *trans* to Se), 34.2 (s, P *trans* to N) ppm.

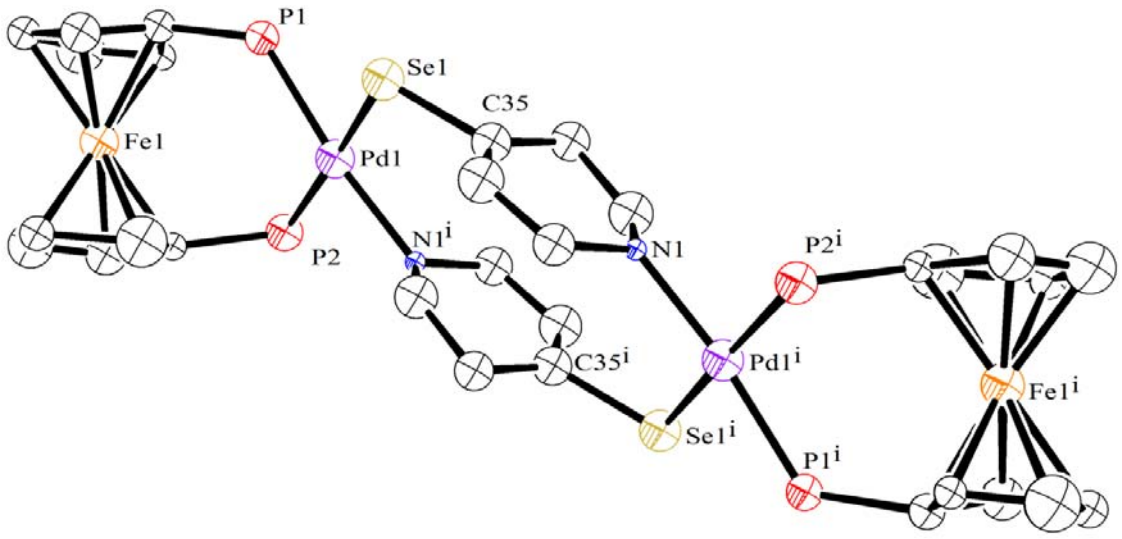

Fig. S12 ORTEP diagram of $[Pd(dppf)(4\text{-}Sepy)]_2(BPh_4)_2$ (**5**) ellipsoids drawn at 35% probability. The dppf phenyl groups, hydrogen atoms and BPh_4 groups are omitted for clarity.

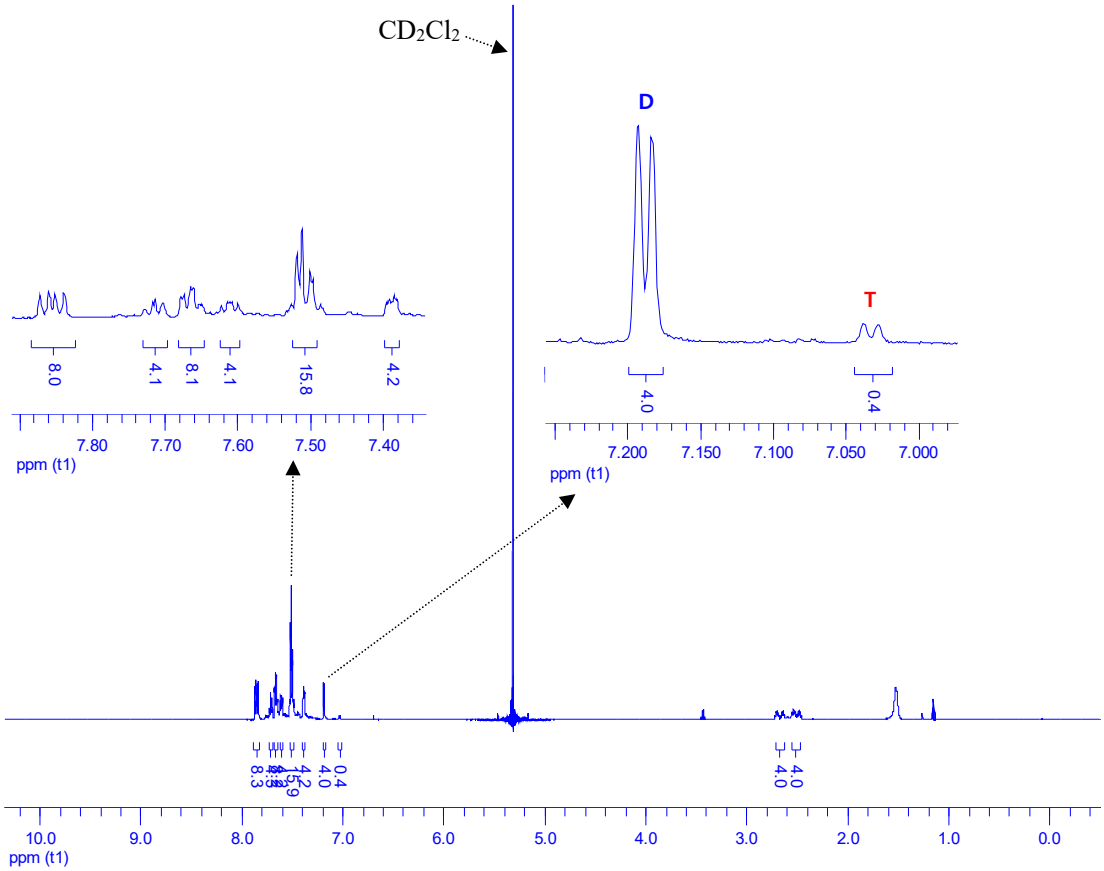

Fig. S13 ^{1}H NMR (600 MHz, CD_2Cl_2, 298 K) spectra of **6**. δ: 2.45-2.58 (m, 4H, CH_2), 2.61-2.74 (m, 4H, CH_2), 7.18 (d, $^{3}J_{H,H}$ = 6.0 Hz, 4H, Hβ-Py, dimer), 7.38 (br m, 4H, Hα-Py), 7.47-7.55 (m, 16H, *m*-H of Ph + *o*-H of Ph), 7.58-7.63 (m, 4H, *p*-H of Ph), 7.67 (dt, $^{3}J_{H,H}$ = 7.5 Hz, $^{4}J_{P,H}$ = 2.5 Hz, 8H, *m*-H of Ph), 7.71 (t, $^{3}J_{H,H}$ = 7.5 Hz, 4H, *p*-H of Ph), 7.86 (dd, $^{3}J_{P,H}$ = 12.6 Hz, $^{3}J_{H,H}$ = 7.5 Hz, 8H, *o*-H of Ph). A peak at δ 7.03 (d, $^{3}J_{H,H}$ = 6.0 Hz, 4H, Hβ-Py) is assigned to the tetramer with the ratio 9:91 with the dimer. All other signals for dimer and tetramer are overlapped.

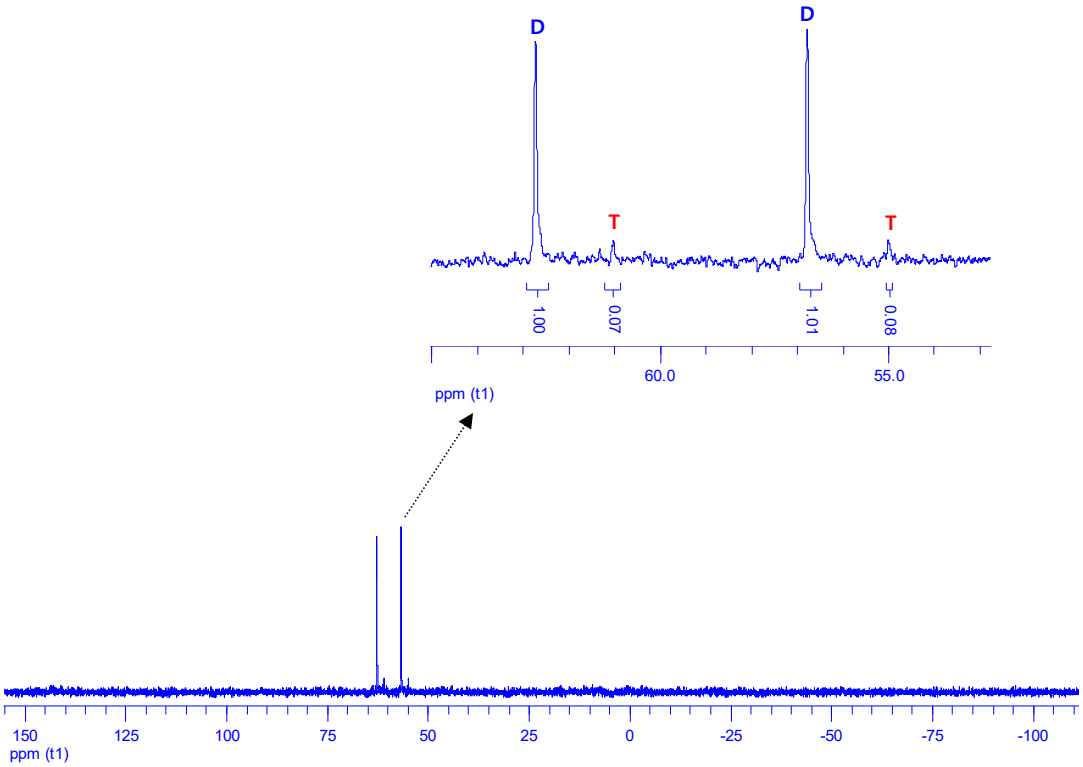

Fig. S14 $^{31}P\{^{1}H\}$ NMR (243 MHz, CD_2Cl_2, 298 K) spectra of **6**. δ: dimer, 56.8 (s, P *trans* to Se), 62.7 (s, P *trans* to N); tetramer, 55.1 (s, P *trans* to Se), 61.0 (s, P *trans* to N) ppm, in 93:7 ratio.

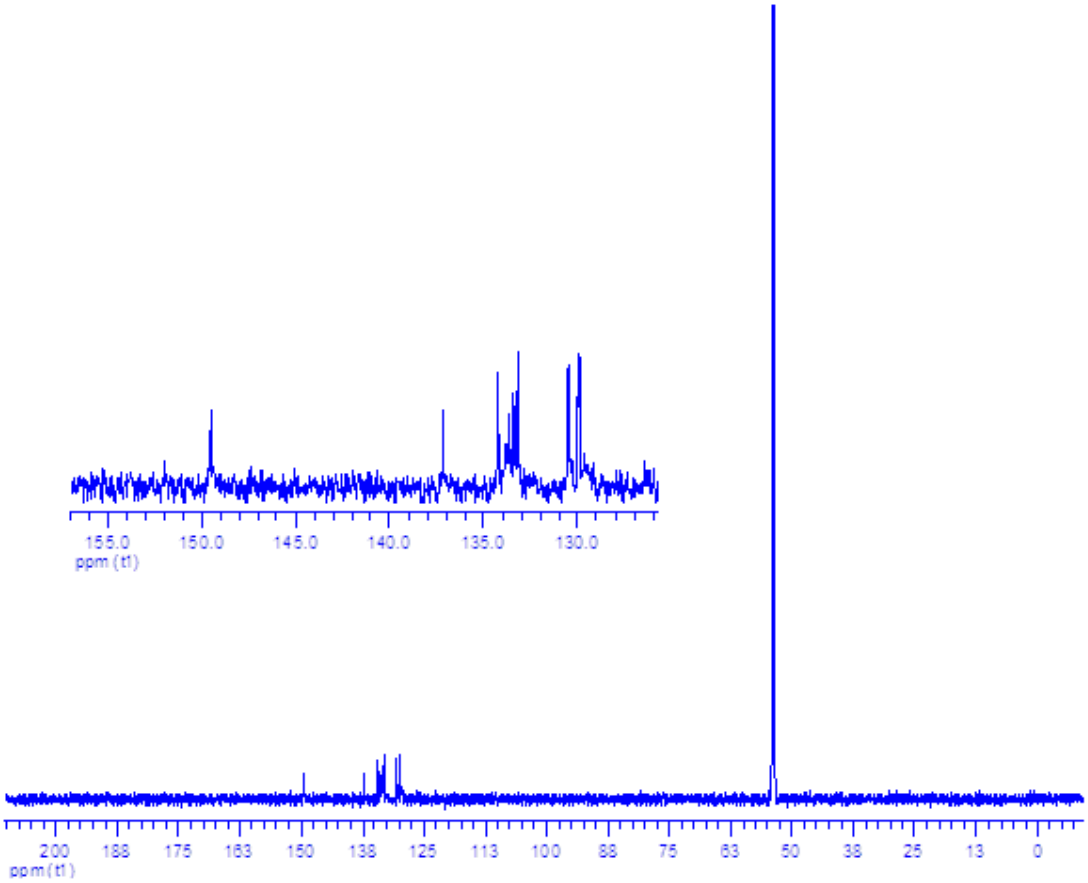

Fig. S15 $^{13}C\{^{1}H\}$ NMR (201 MHz, CD_2Cl_2, 298 K) spectra of **6**. δ: 129.9 (d, $^{3}J_{C,P}$ = 10.1 Hz, *m*-C of Ph); 130.5 (d, $^{2}J_{C,P}$ = 12.1 Hz, *o*-C of Ph); 133.2 (d, $^{3}J_{C,P}$ = 10.1 Hz, *m*-C of Ph); 133.4 (s, *p*-C of Ph); 133.6 (s, *β*-C of Py); 133.8 (m, two i*pso*-C of Ph are merged); 134.3 (d, $^{2}J_{C,P}$ = 12.1 Hz, *o*-C of Ph); 137.2 (s, *p*-C of Ph); 149.5 (s, *α*-C of Py), 152.0 (s, i*pso*-C of Py).

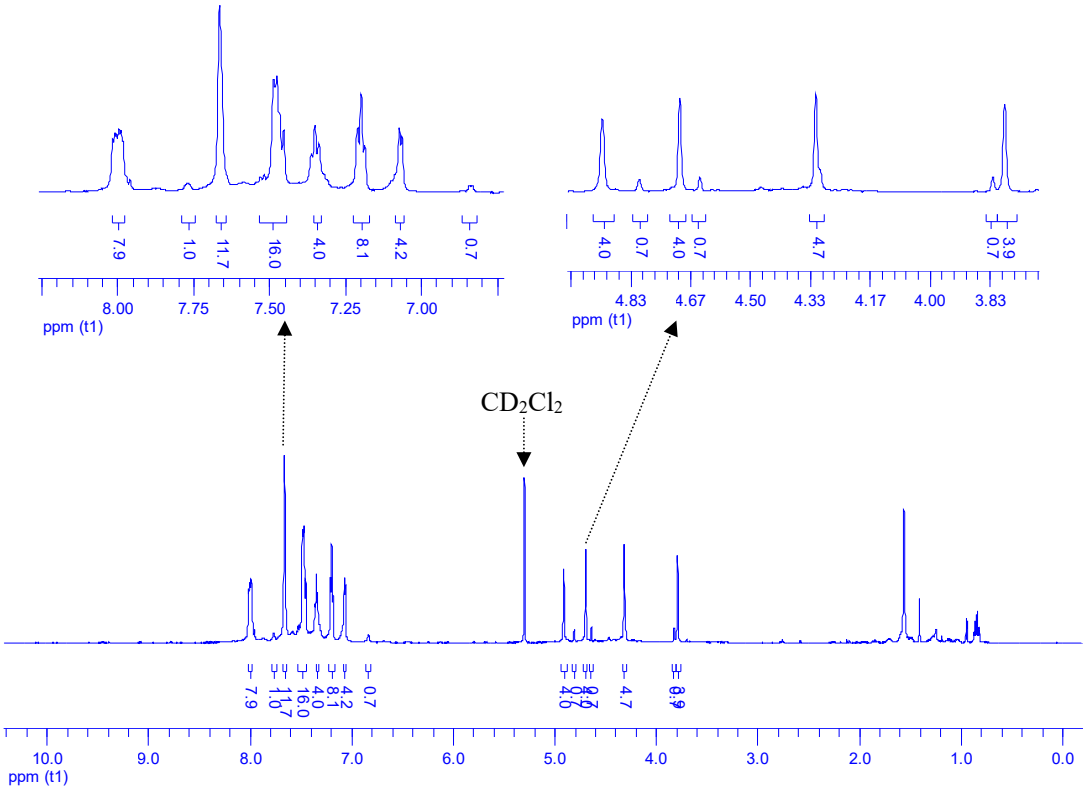

Fig. S16 ^{1}H NMR (600 MHz, CD_2Cl_2, 298 K) spectra of crude product of **7.** The reaction was performed in CH_2Cl_2. δ: dimer, 3.81; tetramer 3.85 (s, 4H, 85:15, H$_\beta$-ferr), tetramer, 4.33; dimer, 4.34 (s, 4H, H$_\beta$-ferr), tetramer, 4.66; dimer, 4.72 (s, 4H, 16:84, H$_\alpha$-ferr); tetramer, 4.83; dimer, 4.93 (s, 4H, 15:85, H$_\alpha$-ferr), tetramer, 6.86; dimer, 7.09 (d, $^{3}J_{H,H}$ = 6 Hz, 4H, H$_\beta$-Py), 7.22 (t, $^{3}J_{H,H}$ = 6 Hz, 8H, *m*-H of Ph), 7.37 (t, $^{3}J_{H,H}$ = 6 Hz, 4H, *p*-H of Ph), 7.49 (m, 16H, *o*-H of Ph + *m*-H of Ph), 7.69 (br s, 12H, *p*-H of Ph + H$_\alpha$-Py), tetramer, 7.79 (br s, 4H, H$_\alpha$-Py), 8.02 (m, 8H, *o*-H of Ph).

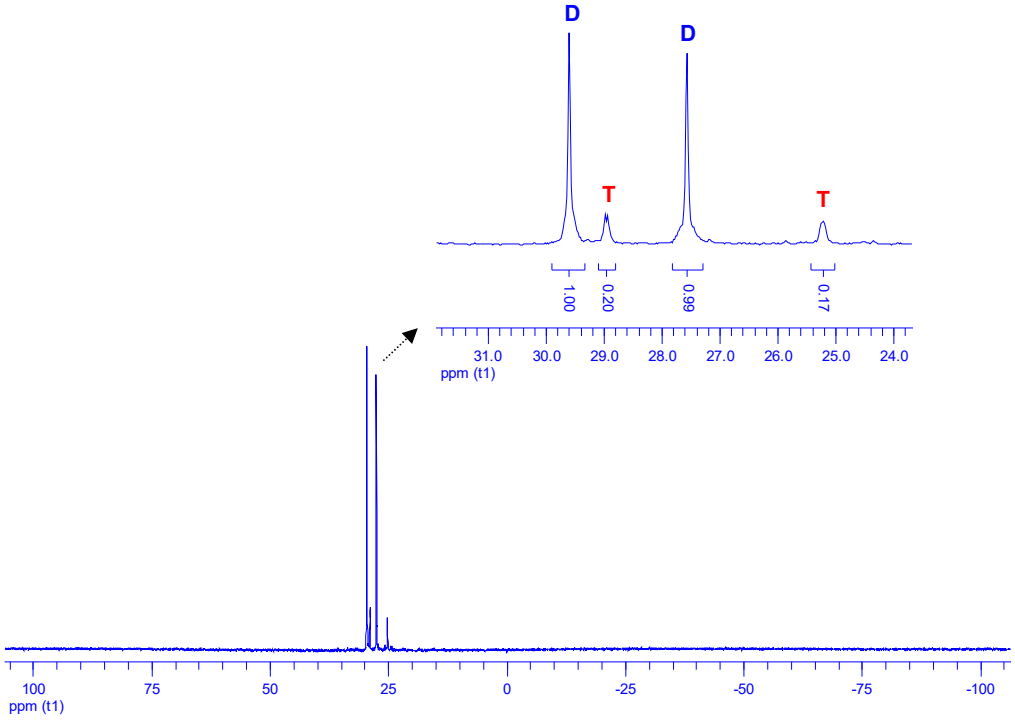

Fig. S17 $^{31}P\{^{1}H\}$ NMR (243 MHz, CD_2Cl_2, 298 K) spectra of crude product of **7.** The reaction was performed in CH_2Cl_2. δ: Tetramer, 25.2 (s), 28.9 (s); Dimer 27.6 (s), 29.6 (s) in 15:85 ratio.

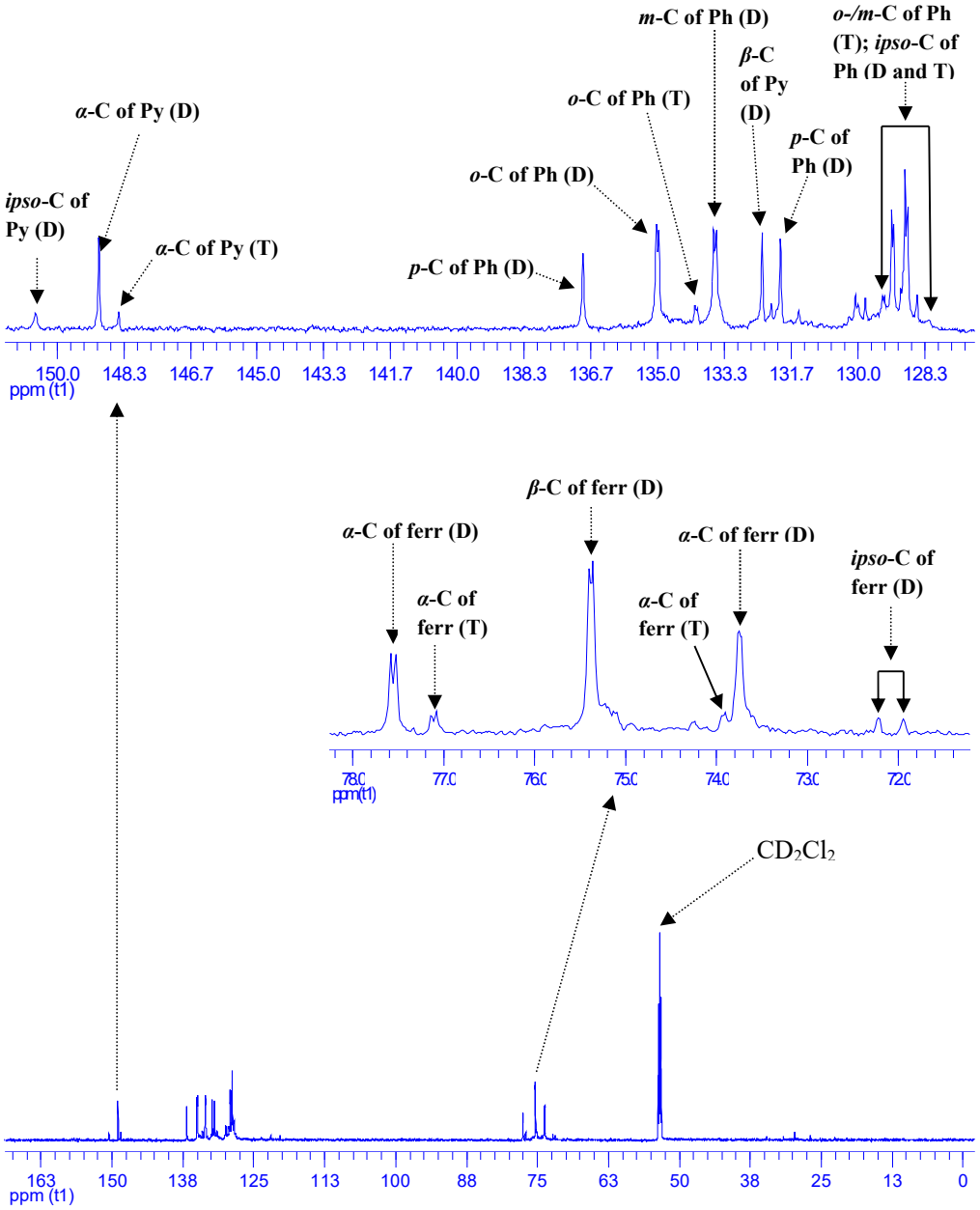

Fig. S18. $^{13}C\{^{1}H\}$ NMR (201 MHz, CD_2Cl_2, 298 K) spectra of **7.** δ: 72.5 (d, $^{1}J_{P\text{-}C}$ = 54.3 Hz, *ipso*-C of ferr, D); 74.2 (d, $^{2}J_{P,C}$ = 8.0 Hz, *α*-C of ferr, D); 74.3 (d, $^{2}J_{P,C}$ = 8.0 Hz, *α*-C of ferr, T); 75.5, 75.6 (each d, $^{2}J_{P,C}$ = 8.0 Hz, *β*-C of ferr, T); 75.8 (d, $^{3}J_{P,C}$ = 8.0 Hz, *β*-C of ferr, D); 77.5 (d, $^{2}J_{P,C}$ = 10.1 Hz, *α*-C of ferr, T); 77.9 (d, $^{2}J_{P,C}$ = 10.1 Hz, *α*-C of ferr, D); 128.9 (s); 129.2 (d, $^{3}J_{P,C}$ = 10.1 Hz, *m*-C of Ph, D); 129.5 (d, $^{2}J_{P,C}$ = 10.1 Hz, *o*-C of Ph, D); 129.3 (s), 129.8 (d, *J* = 10.1 Hz), 130.2 (s), 130.5 (s), 130.6 (s) (*o*-/*m*-C of Ph, T; *ipso*-C of Ph, D and T); 131.9 (s, *p*-C of Ph, T); 132.3 (s, *p*-C of Ph, D); 132.6 (s, *β*-C of Py, T); 132.8 (s, *β*-C of Py, D); 133.9 (d, $^{3}J_{P,C}$ = 12.1 Hz, *m*-C of Ph, D), 134.4 (d, $^{2}J_{P,C}$ = 8.1 Hz, *o*-C of Ph, T); 135.4 (d, $^{2}J_{P,C}$ = 10.1 Hz, *o*-C of Ph, D); 137.3 (s, *p*-C of Ph, D); 148.9, 149.4 (each s, *α*-C of Py, D, T); 150.9 (s, *ipso*-C of Py, D).

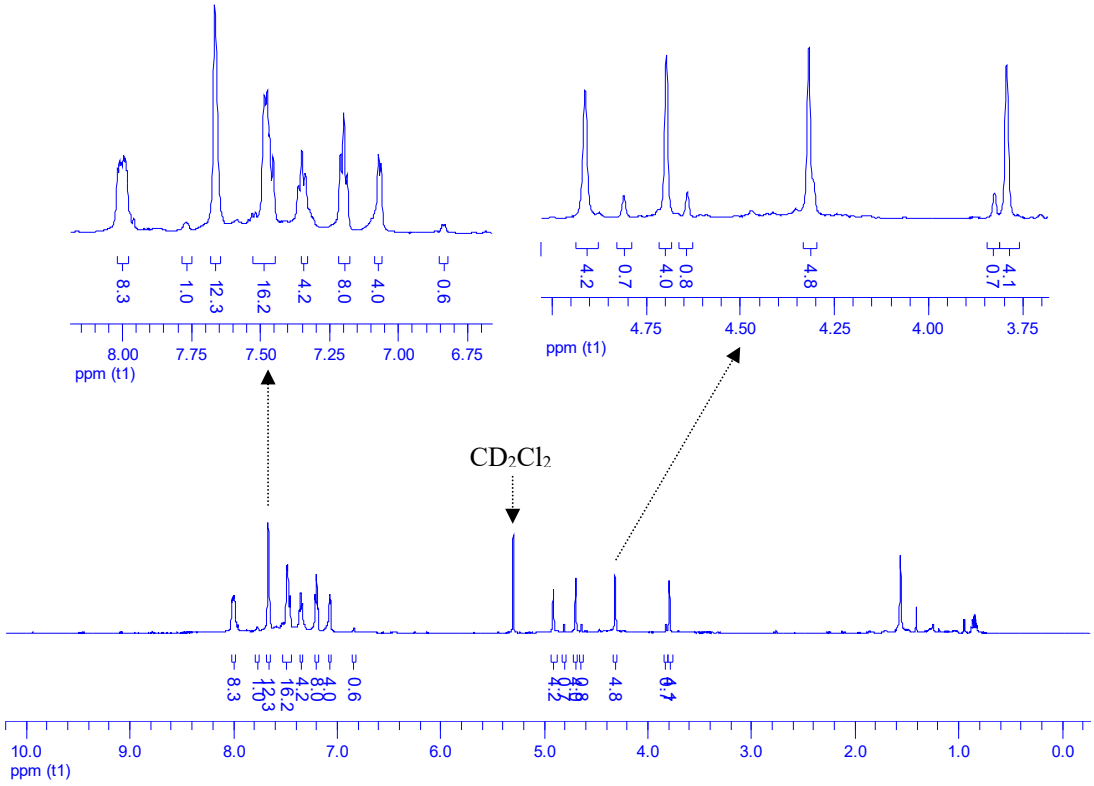

Fig. S19 ^{1}H NMR (600 MHz, CD_2Cl_2, 298 K) spectra of recrystallized product of **7**. The reaction was performed in acetone**.** δ: dimer, 3.81; tetramer 3.85 (s, 4H, 85:15, H$_\beta$-ferr), tetramer, 4.33; dimer, 4.34 (s, 4H, H$_\beta$-ferr), tetramer, 4.66; dimer, 4.72 (s, 4H, 16:84, H$_\alpha$-ferr); tetramer, 4.83; dimer, 4.93 (s, 4H, 15:85, H$_\alpha$-ferr), tetramer, 6.86; dimer, 7.09 (d, $^{3}J_{H,H}$ = 6 Hz, 4H, H$_\beta$-Py), 7.22 (t, $^{3}J_{H,H}$ = 6 Hz, 8H, *m*-H of Ph), 7.37 (t, $^{3}J_{H,H}$ = 6 Hz, 4H, *p*-H of Ph), 7.49 (m, 16H, *o*-H of Ph + *m*-H of Ph), 7.69 (br s, 12H, *p*-H of Ph + H$_\alpha$-Py), tetramer, 7.79 (br s, 4H, H$_\alpha$-Py), 8.02 (m, 8H, *o*-H of Ph).

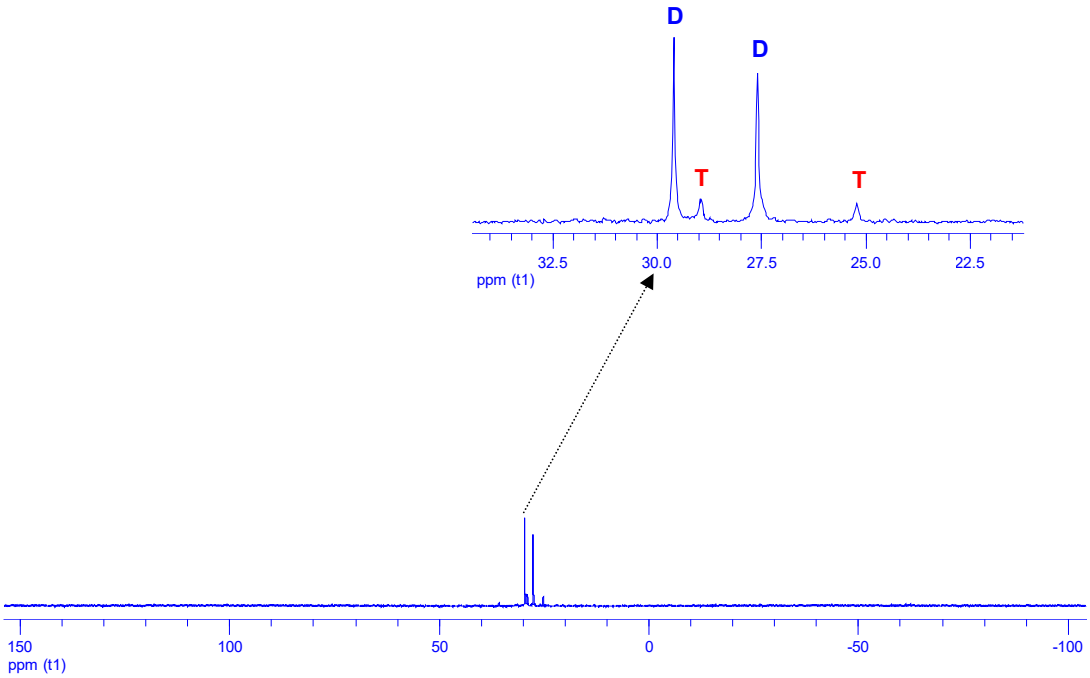

Fig. S20 $^{31}P\{^{1}H\}$ NMR (243 MHz, CD_2Cl_2, 298 K) spectra of recrystallized product of **7**. The reaction was performed in acetone**.** δ: Tetramer, 25.2 (s), 28.9 (s); Dimer 27.6 (s), 29.6 (s) in 15:85 ratio.

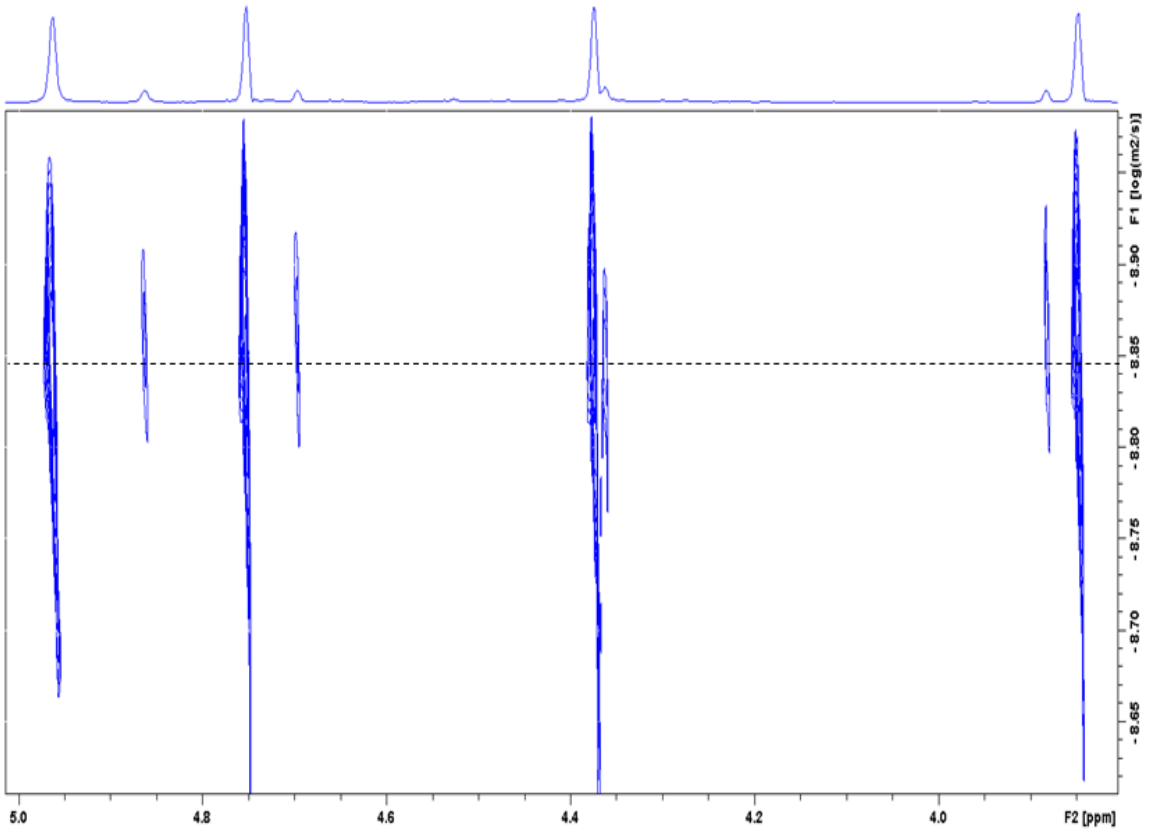

Fig. S21. The ^{1}H DOSY NMR (800 MHz, CD_2Cl_2, 298 K) spectrum of **7a/b**.

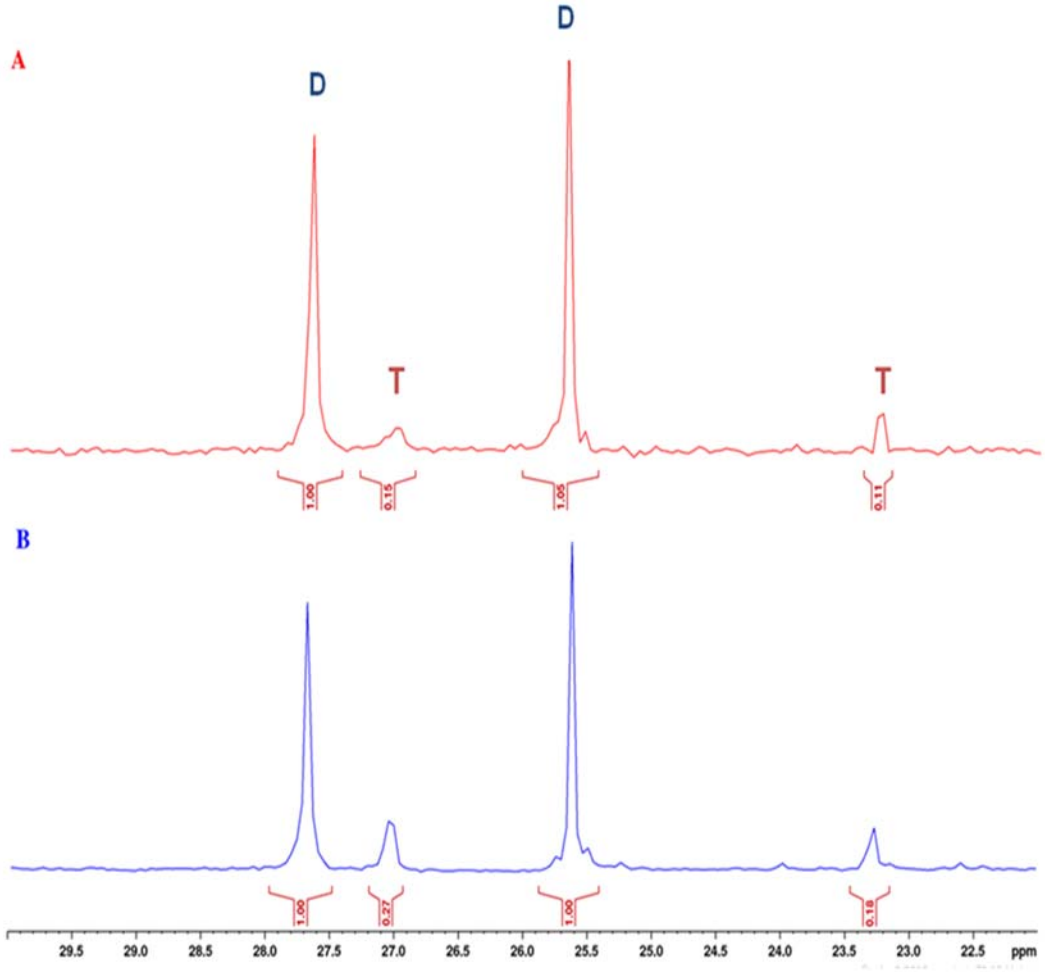

Fig. S22. $^{31}P\{^{1}H\}$ NMR spectra (243 MHz, CD_2Cl_2, 298 K) of **7. (A)** 7.1 mg/500 μL; (**B**) 34.7 mg/500 μL.

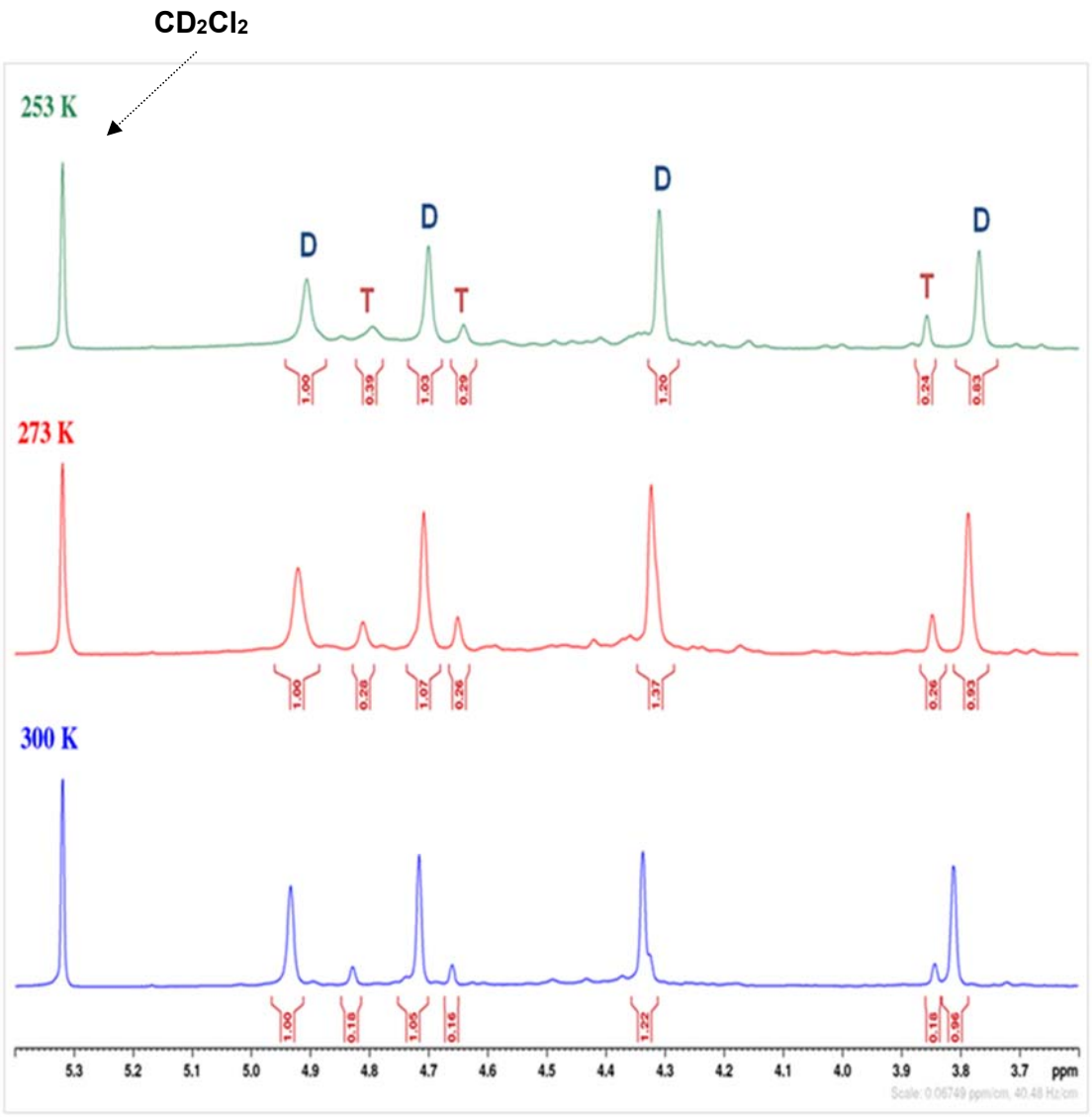

Fig. S23. Variable-temperature ^{1}H NMR (600 MHz, CD_2Cl_2) spectra of **7**.

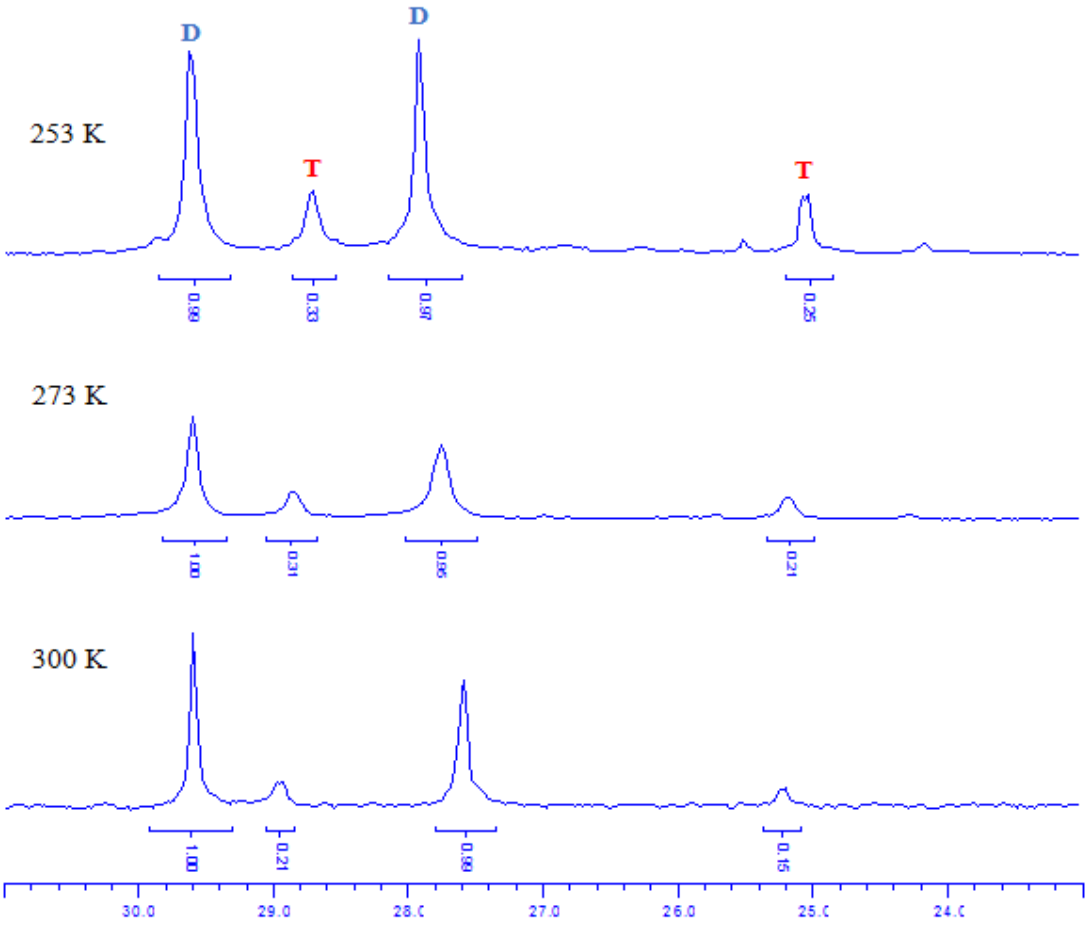

Fig. S24. Variable-temperature $^{31}P\{^{1}H\}$ NMR (243 MHz, CD_2Cl_2) spectra of **7.**

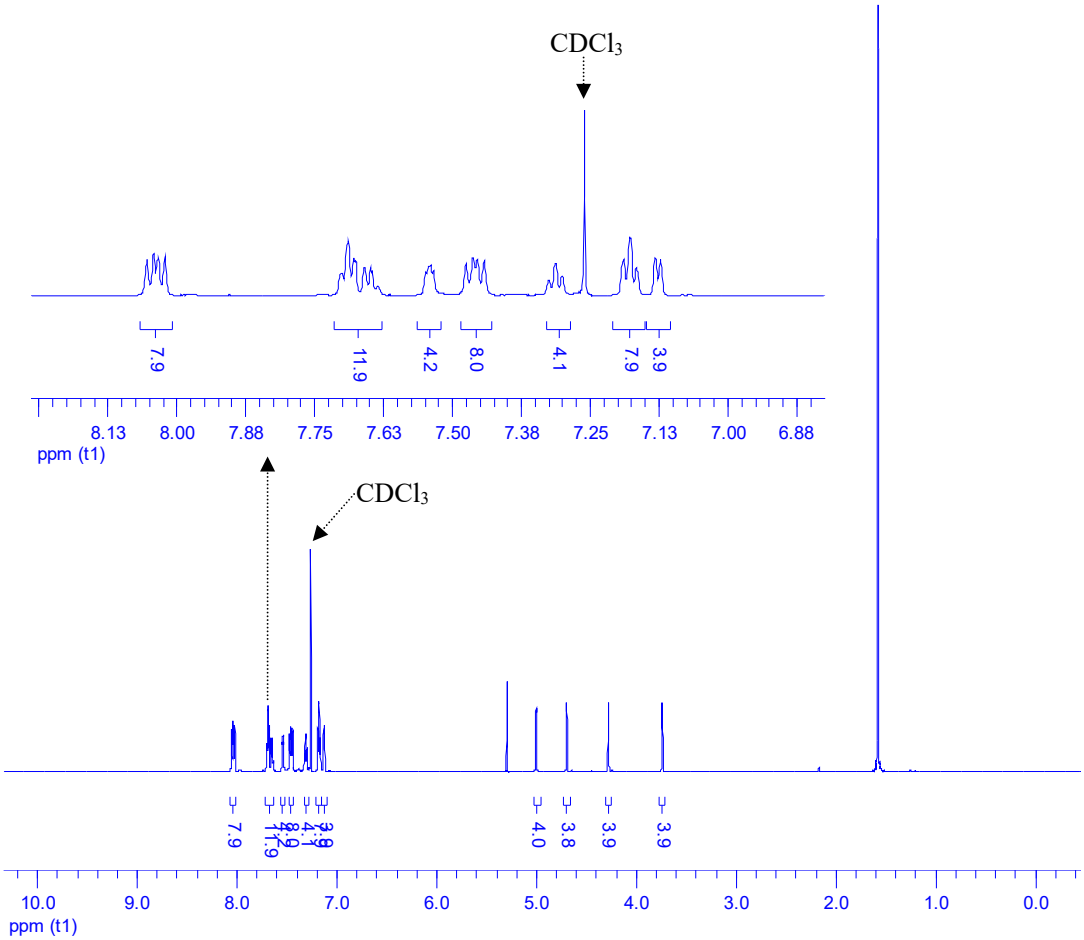

Fig. S25 ^{1}H NMR (600 MHz, $CDCl_3$, 298 K) spectra of **7**. δ: 3.74 (s, 4H, H$_\beta$-ferr), 4.28 (s, 4H, H$_\beta$-ferr), 4.70 (s, 4H, H$_\alpha$-ferr), 5.00 (s, 4H, H$_\alpha$-ferr), 7.13 (d, $^{3}J_{H,H}$ = 5.6 Hz, 4H, H$_\beta$-py), 7.18 (dt, $^{3}J_{H,H}$ = 7.5 Hz, $^{4}J_{P,H}$ = 1.9 Hz, 8H, *m*-H of Ph), 7.31 (t, $^{3}J_{H,H}$ = 7.5 Hz, 4H, *p*-H of Ph), 7.46 (dd, $^{3}J_{P,H}$ = 12.5 Hz, $^{3}J_{H,H}$ = 7.5 Hz, 8H, *o*-H of Ph), 7.54 (dd, $^{3}J_{H,H}$ = 5.6 Hz, $^{4}J_{P,H}$ = 3.1 Hz, 4H, H$_\alpha$-py), 7.63-7.67 (m, 4H, *p*-H of Ph), 7.69 (t, $^{3}J_{H,H}$ = 7.8 Hz, 8H, *m*-H of Ph), 8.04 (dd, $^{3}J_{P,H}$ = 12.5 Hz, $^{3}J_{H,H}$ = 7.5 Hz, 8H, *o*-H of Ph).

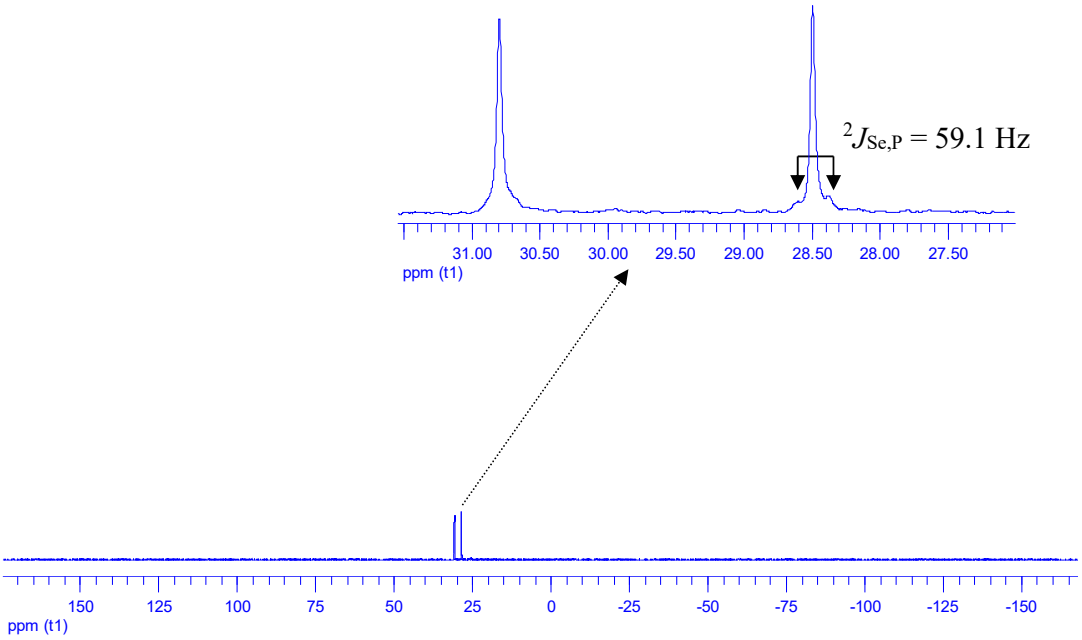

Fig. S26 $^{31}P\{^1H\}$ NMR (121 MHz, $CDCl_3$, 298 K) spectra of **7**. δ: 28.5 (s, $^2J_{Se,P}$ = 59.1 Hz, P *trans* to Se), 30.8 (s, P *trans* to N).

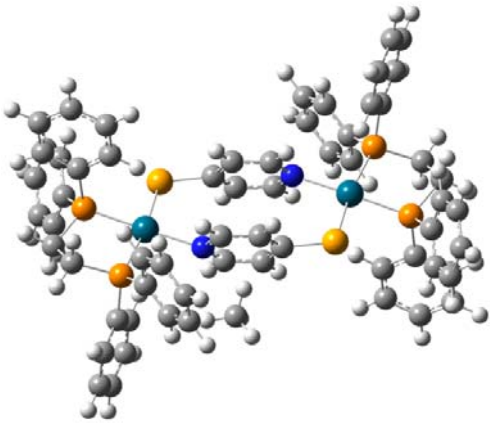

6a

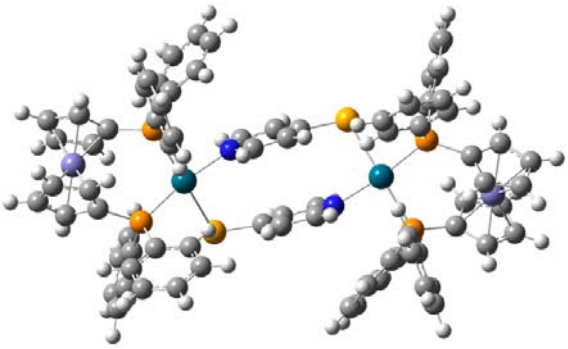

7a

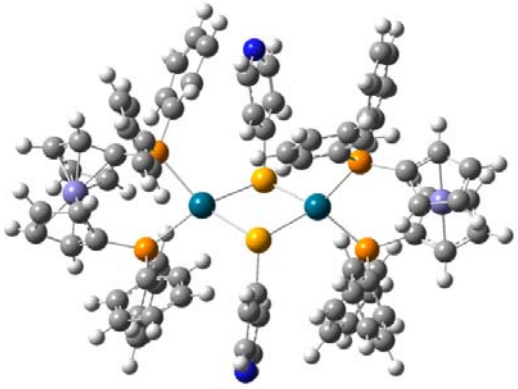

7′

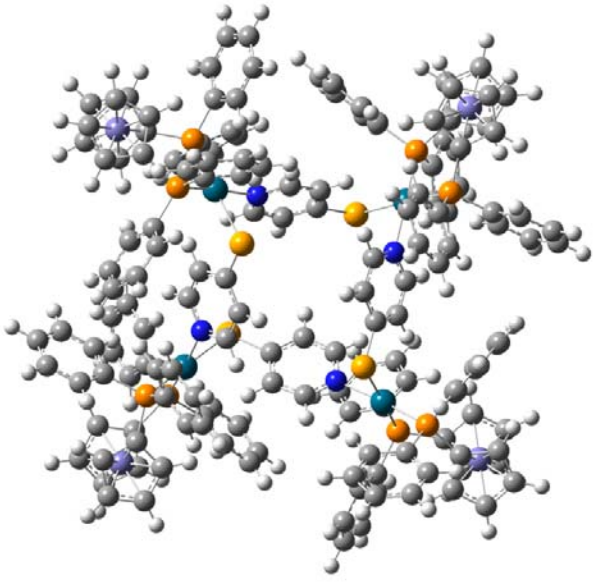

7b

Fig. S27 Optimized minimum energy structures calculated applying DFT method.

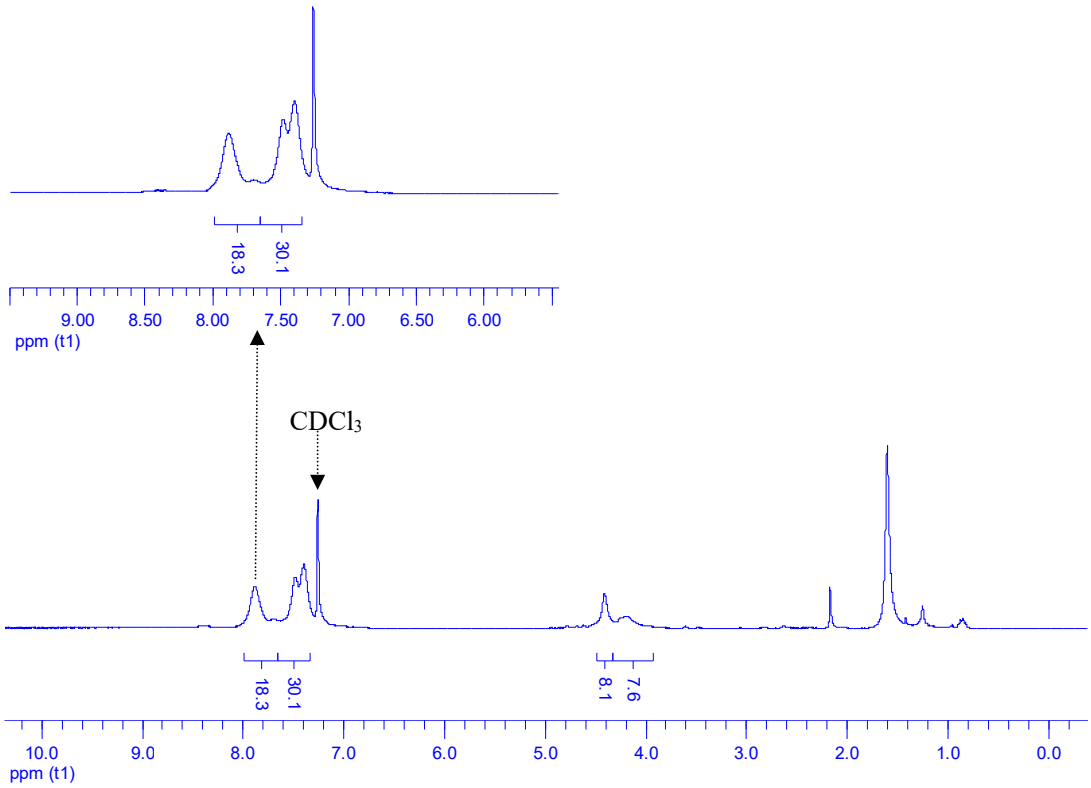

Fig. 28 ^{1}H NMR (300 MHz, $CDCl_3$, 298 K) spectra of **8**. δ: 4.19 (br s, 8H, H_{β}-ferr), 4.41 (s, 8H, H_{α}-ferr), 7.40 (br s, 16H, *m*-H of Ph), 7.49 (br s, 8H, *p*-H of Ph), 7.89 (br s, 16H, *o*-H of Ph), the peaks correspond to the 4H of H_{β}-py and H_{α}-py each merged in the base.

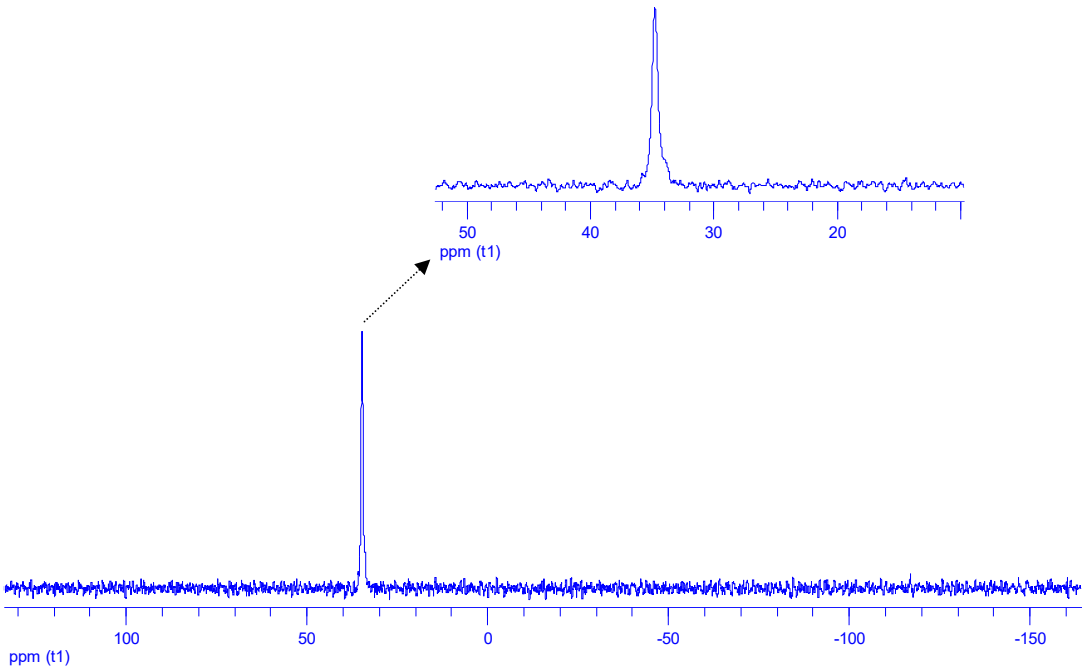

Fig. 29 $^{31}P\{^{1}H\}$ NMR (121 MHz, $CDCl_3$, 298 K) spectra of **8**. δ: 34.8 (s) ppm.

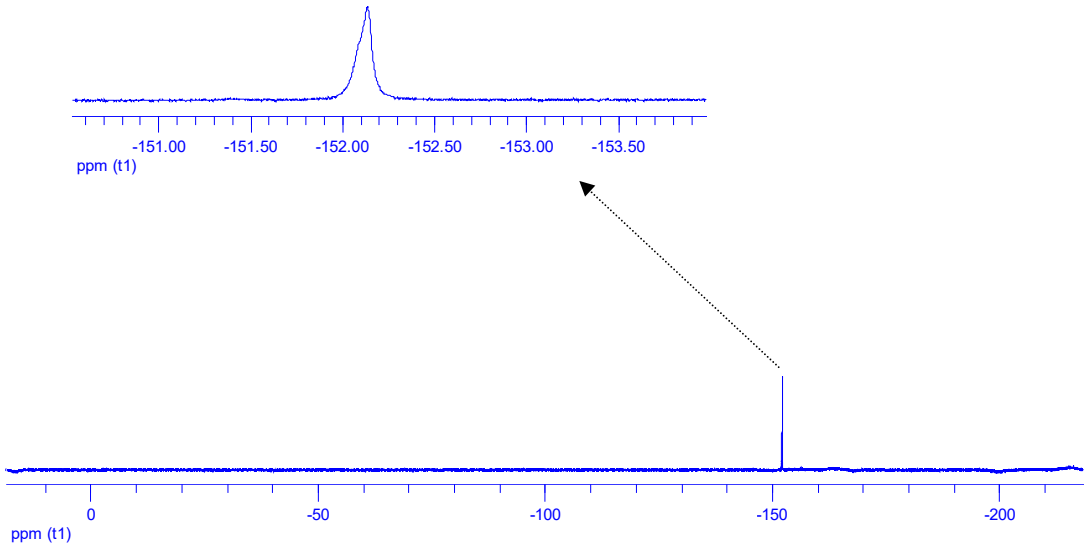

Fig. 30 $^{19}F\{^{1}H\}$ NMR (282 MHz, $CDCl_3$, 298 K) spectra of **8**. δ: −152.07 (br, $^{10}BF^-$), −152.12 (br s, $^{11}BF^-$) ppm.

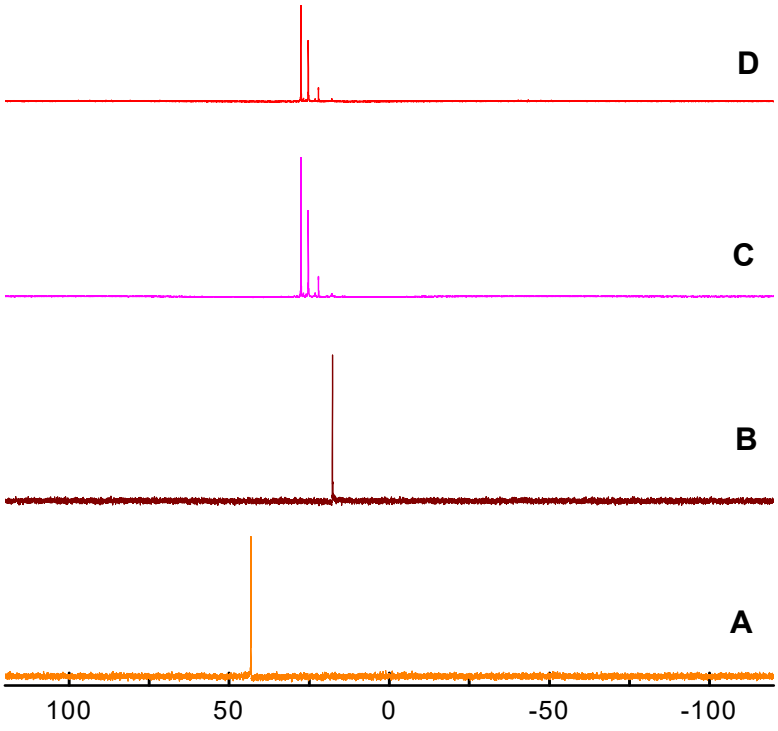

Fig. S31 ^{31}P NMR (243 MHz, $CDCl_3$, 298 K) spectra obtained from mixture of $Pd(dppf)(OTf)_2$ and **2** in 1:1 ratio in NMR tube. (**A)** only $Pd(dppf)(OTf)_2$; (**B**) only $Pd(dppf)(4\text{-}Sepy)_2$; (**C**) immediately after addition; (**D**) after 2 days.

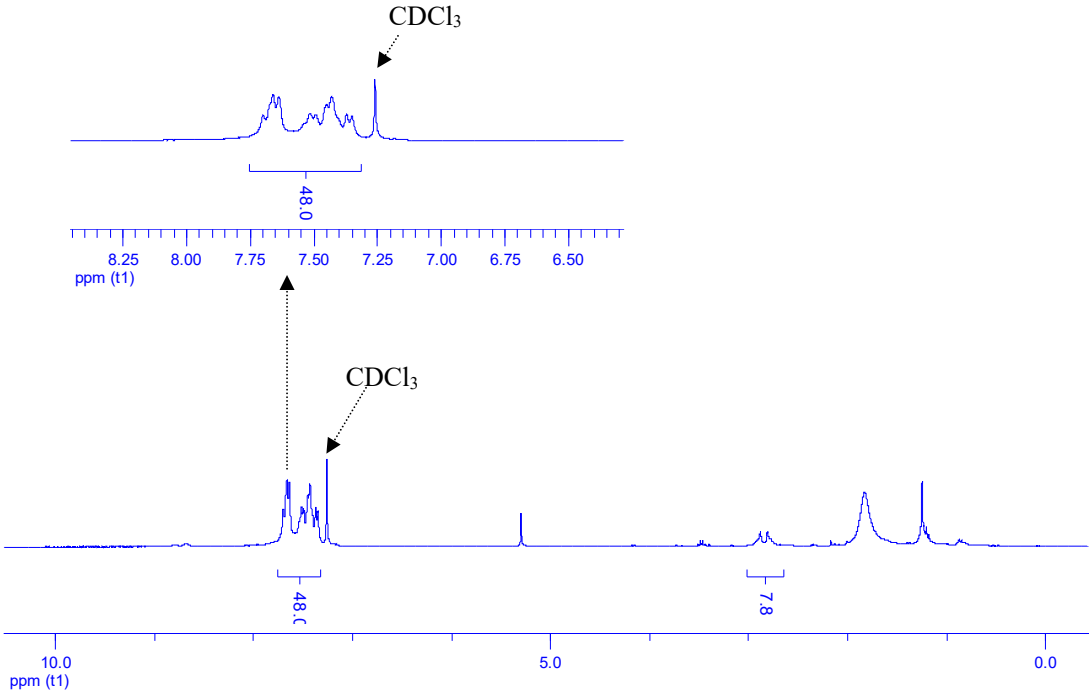

Fig. S32 ^{1}H NMR (300 MHz, $CDCl_3$, 298 K) spectra of **9**. δ: 2.63 (d, $^{2}J_{P,H}$ = 22.9 Hz, 8H, CH_2), 7.36-7.76 (m, 48H, Ph + py).

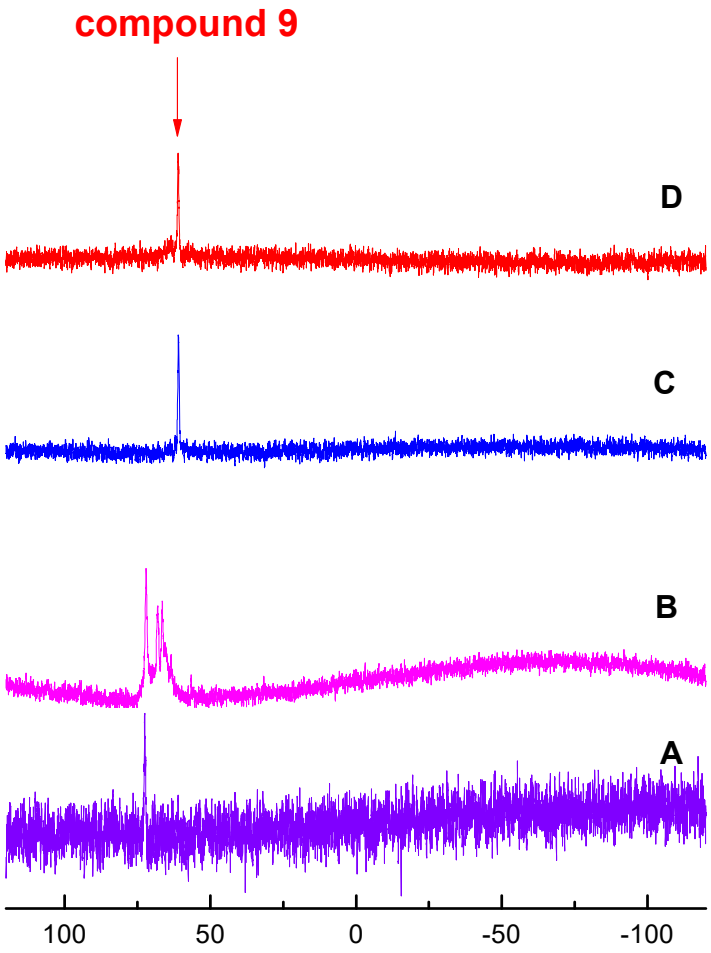

Fig. S33 ^{31}P NMR (121 MHz, $CDCl_3$, 298 K) spectra obtained from mixture of $Pd(dppe)(OTf)_2$ and 4-pySH in 1:1 ratio in NMR tube. (**A)** only $Pd(dppe)(OTf)_2$; (**B**) immediately after addition; (**C**) after 1 day; (D) after 4 days.

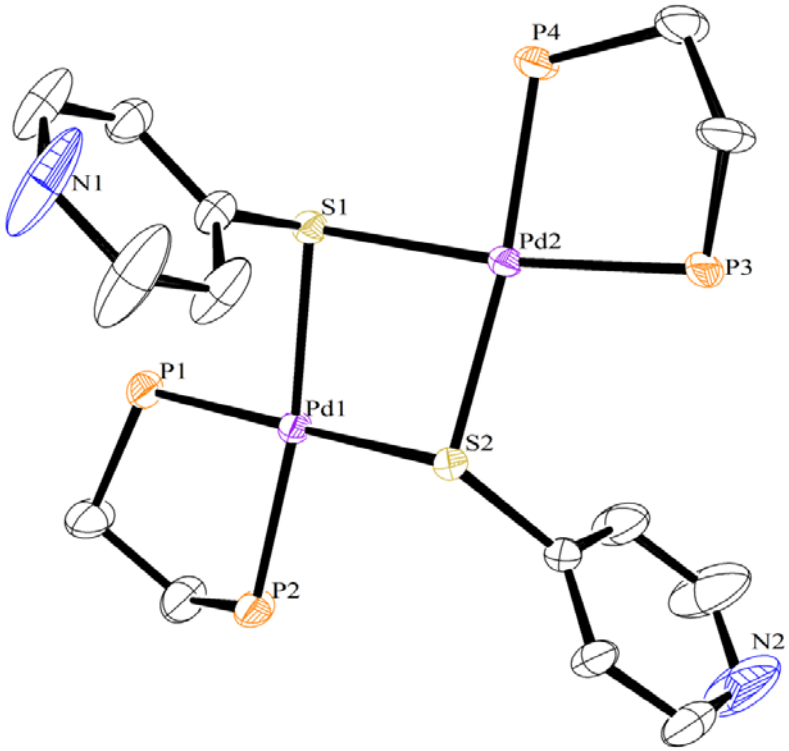

Fig. S34 ORTEP diagram of $[Pd(dppe)(4\text{-}Spy)]_2(OTf)_2 \cdot (CF_3SO_3H)_2 \cdot (CHCl_3)_2 \cdot H_2O$ (**9**$\cdot (CF_3SO_3H)_2 \cdot (CHCl_3)_2 \cdot H_2O$) ellipsoids drawn at 50% probability. The dppe phenyl groups, hydrogen atoms, solvent molecules, triflic acid and triflate ions are omitted for clarity.

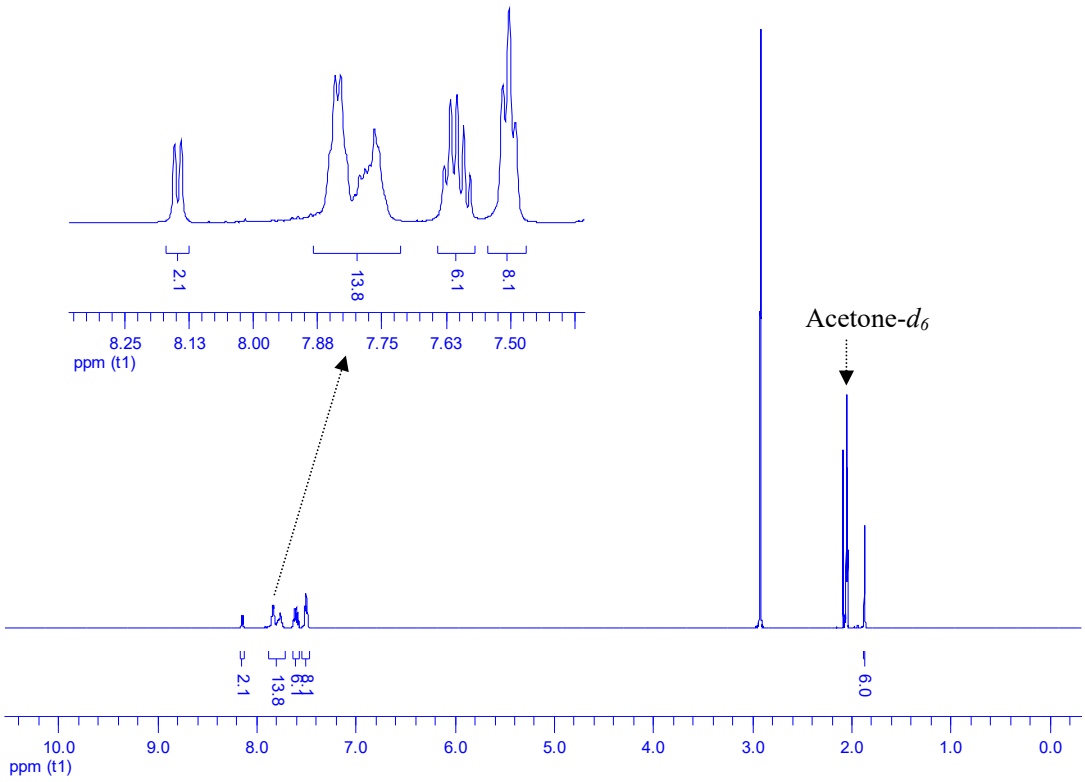

Fig. S35 ^{1}H NMR (600 MHz, acetone-d_6, 298 K) spectra of **10**. δ: 1.87 (s, 6H, CH_3), 7.50 (t, $^{3}J_{H,H}$ = 7.5 Hz, 8H, *m*-H of Ph), 7.56-7.63 (m, 6H, *p*-H of Ph + H_{β}-py), 7.72-7.81 (m, 6H, H_{α}-py + CHC*H*CH + CPC*H*CH), 7.84 (dd, $^{3}J_{P,H}$ = 13.1 Hz, $^{3}J_{H,H}$ = 6.3 Hz, 8H, *o*-H of Ph), 8.14 (d, 7.8 Hz, 2H, CHC*H*CC).

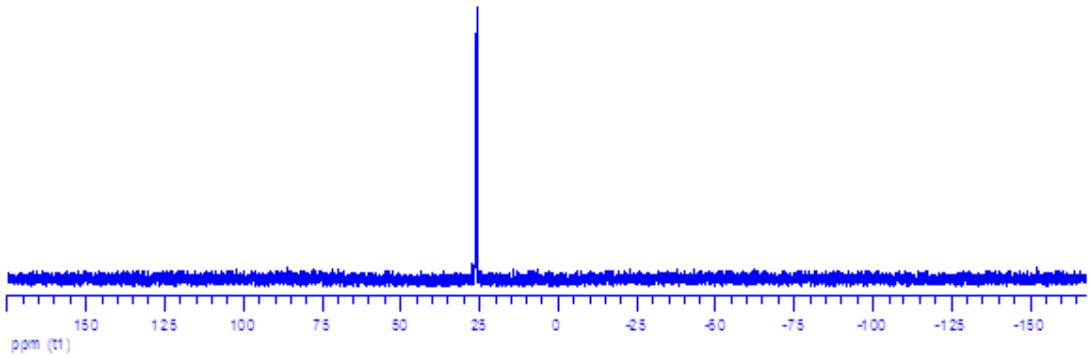

Fig. S36 $^{31}P\{^{1}H\}$ NMR (121 MHz, acetone-*d*$_6$, 298 K) spectrum of **10**. δ 25.9 (s) ppm.

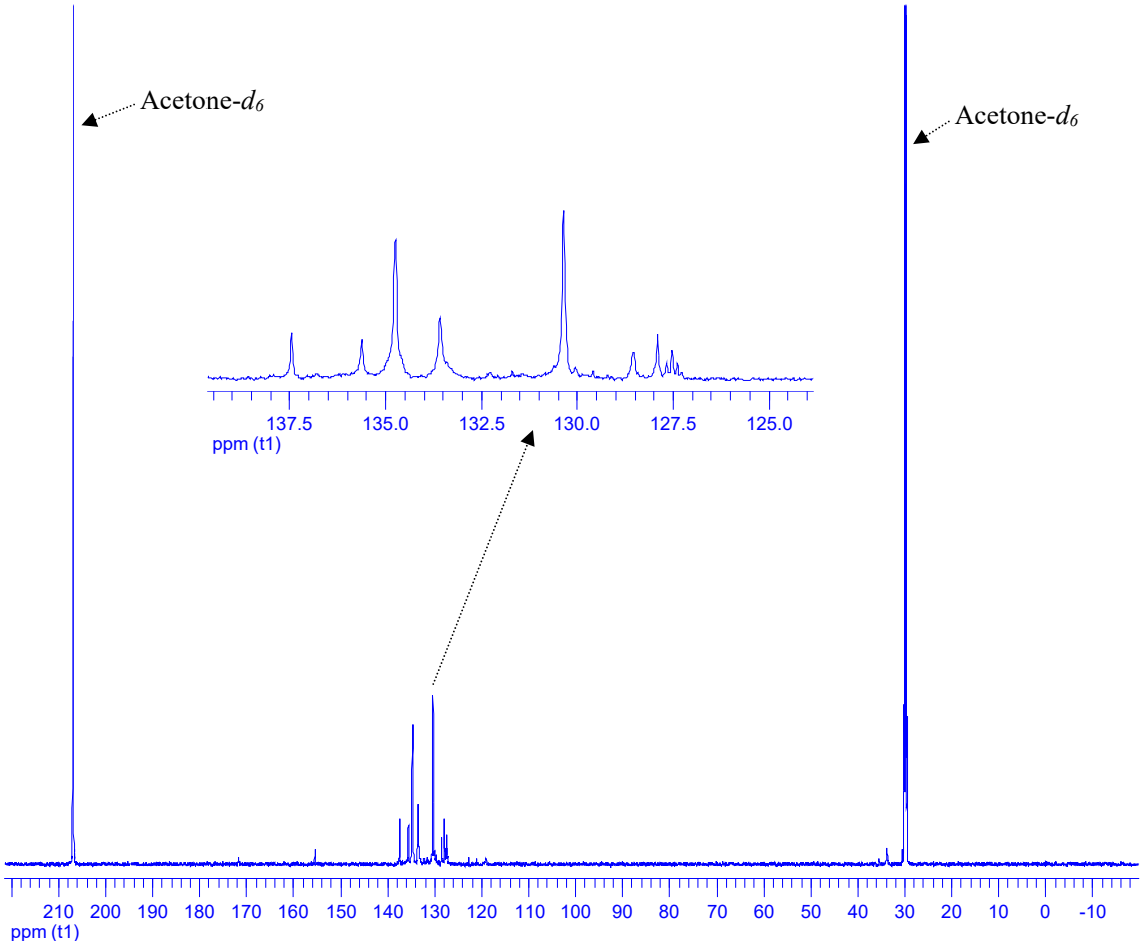

Fig. S37. $^{13}C\{^{1}H\}$ NMR (201 MHz, acetone-d_6, 298 K) spectra of **10**. δ: 33.8 (s, CH_3); 35.4 (s, CCH_3); 127.5 (t, $^{3}J_{P,C}$ = 27.6 Hz, CP of $C_{15}H_{12}O$); 127.9 (s, CH of $C_{15}H_{12}O$); 128.5 (s, CH of $C_{15}H_{12}O$); 130.4 (s, *m*-C of Ph); 133.6 (s, *p*-C of Ph); 134.8 (s, *o*-C of Ph); 135.6 (s, *β*-C of Py); 137.5 (s, CH of $C_{15}H_{12}O$); 155.5 (s, *α*-C of Py); 171.7 (s, CO of $C_{15}H_{12}O$). The peaks correspond to *ipso*-C of Ph and C*C*C(CH_3) are merged with the other peaks.

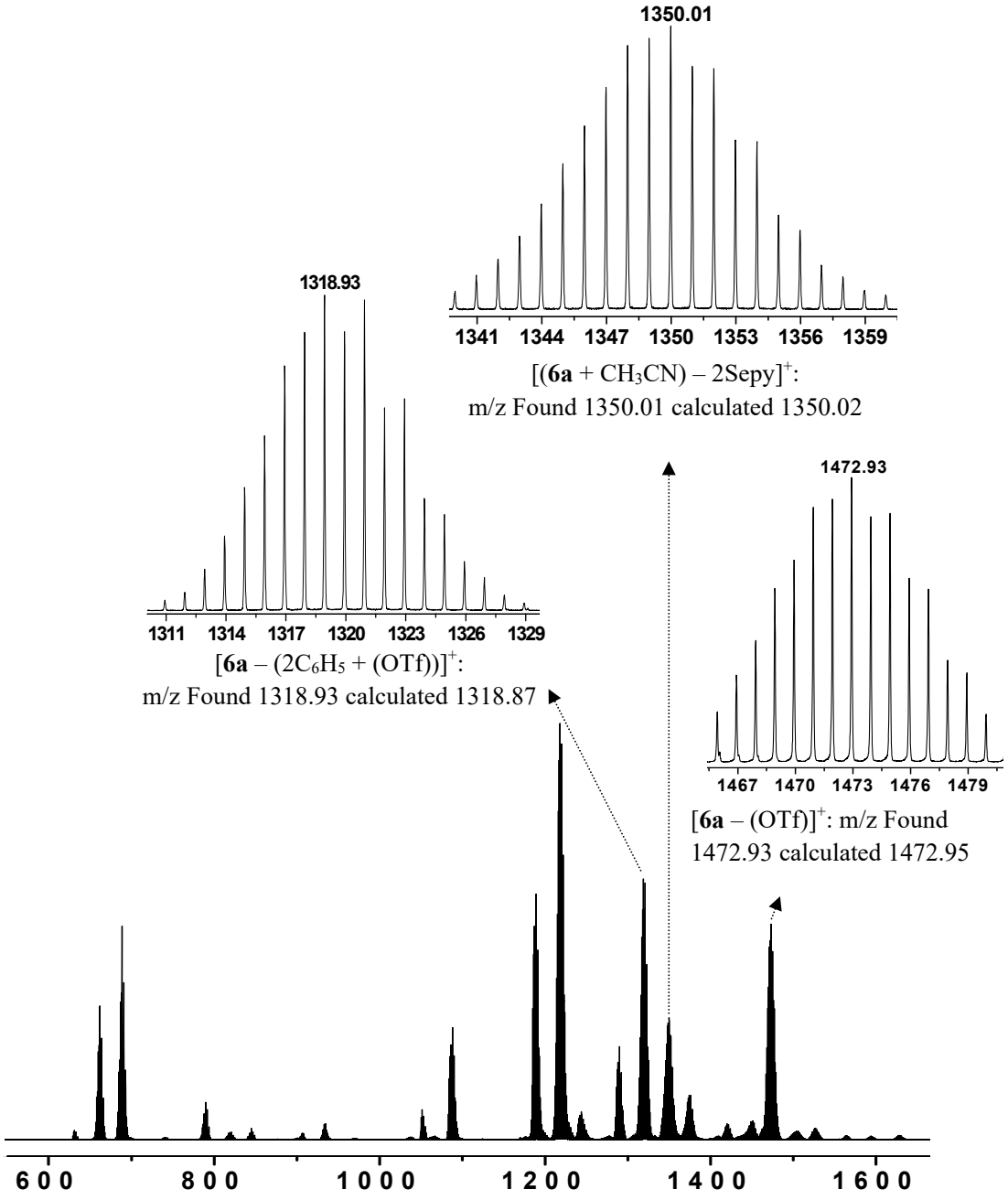

Fig. S38 ESI mass-spectrum of **6**. The insets show the experimentally obtained isotope patterns of the fragments. The found and calculated values are for the most abundant peak of the ion.

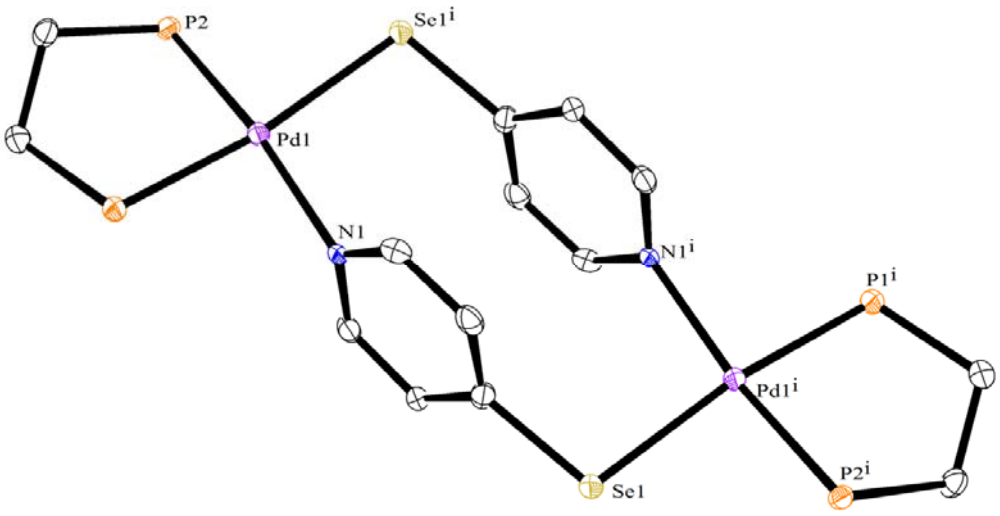

Fig. S39 ORTEP diagram of $[Pd(dppe)(4\text{-}Sepy)]_2(OTf)_2$ (**6a**) ellipsoids drawn at 50% probability. The dppe phenyl groups, hydrogen atoms, and triflate ions are omitted for clarity.

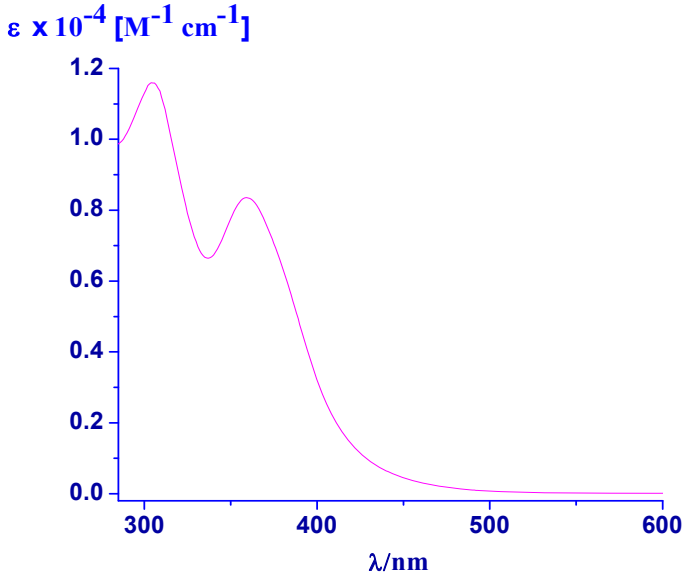

(b)

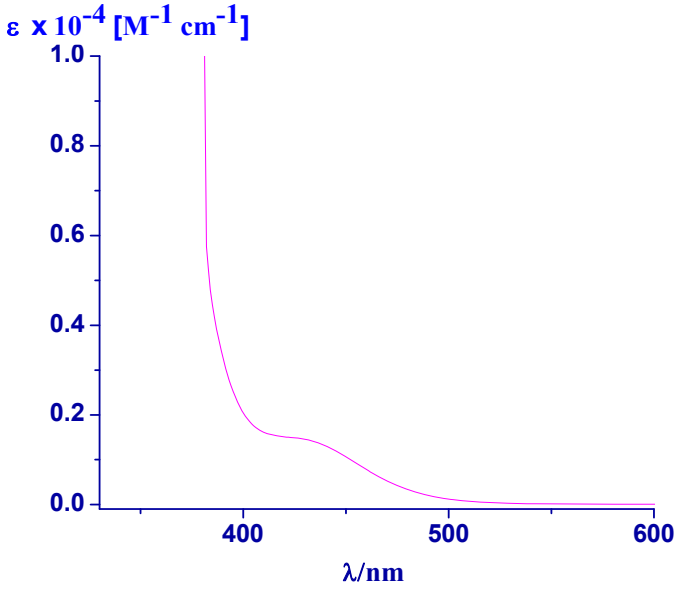

(a)

Fig. S40 UV-vis spectra of **6** in ACN solution, a) stock solution, b) after dilution.

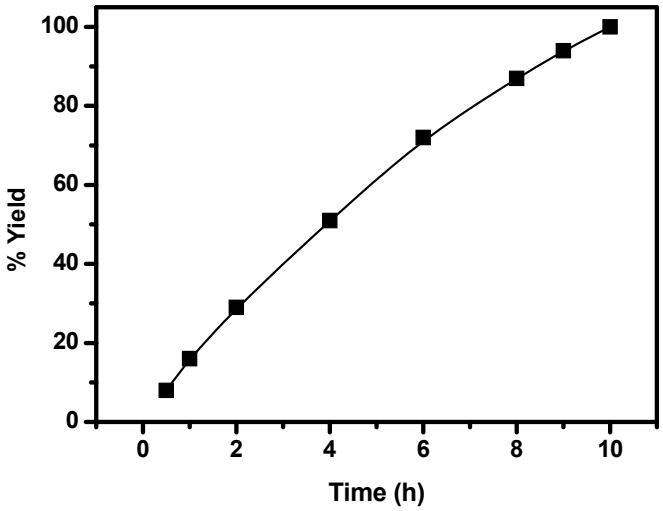

Fig. S41 Plot of time vs yield of the coupling product obtained from the reaction of 4-bromoacetophenone and phenylboronic acid catalyzed by **7.**

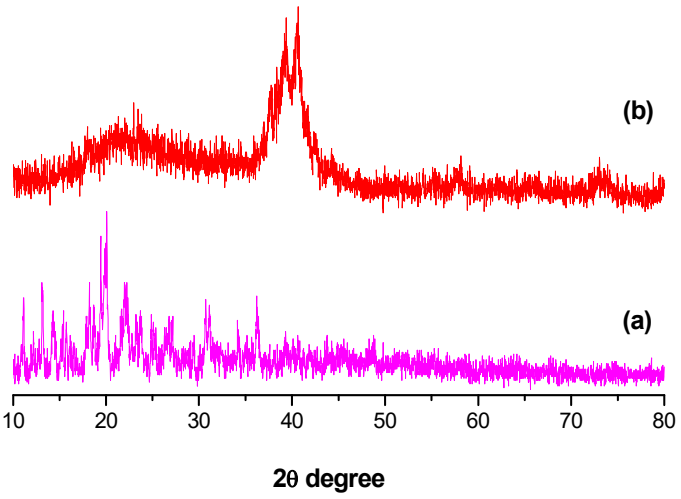

Fig. S42 PXRD patterns of (a) complex **7** before catalysis, (b) compound after catalysis reaction of complex **7**.

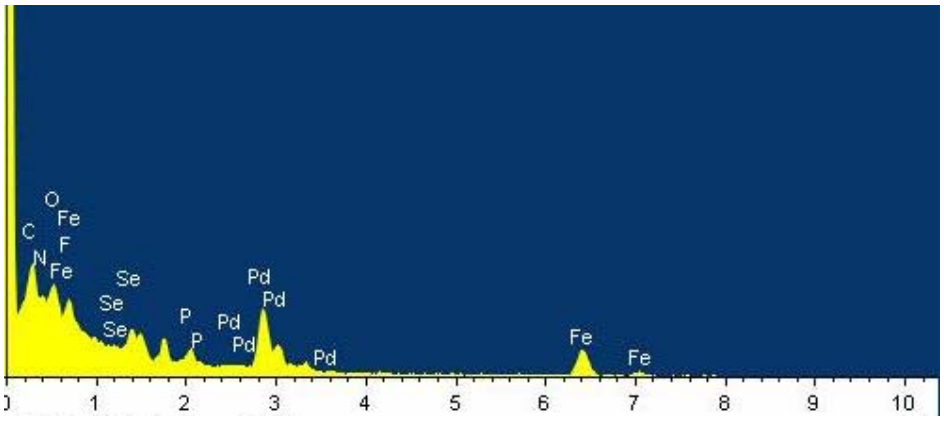

Fig. S43 EDAX spectrum of the compound after catalysis reaction of complex **7**.

Methyl 4– phenyl benzoate: (White solid, M.P. = 117 °C), ^{1}H NMR (500 MHz, $CDCl_3$) δ = 3.95 (s, 3H), 7.40 (t, J = 7.5 Hz, 1H), 7.47 (t, J = 7.5 Hz, 2H), 7.62 (d, J = 7.5 Hz, 2H), 7.66 (d, J = 8.5 Hz, 2H), 8.11 (d, J = 8.0 Hz, 2H).

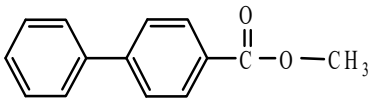

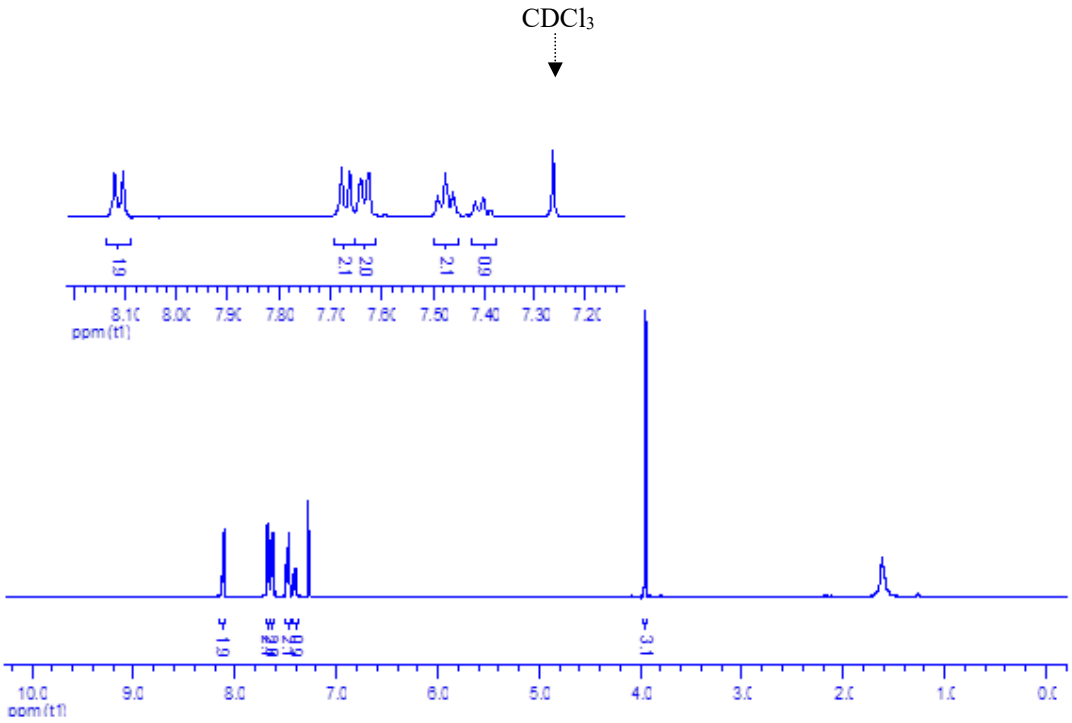

Fig. S44 ^{1}H NMR (500 MHz, $CDCl_3$, 298 K) spectra of methyl 4– phenyl benzoate

2-Phenylthiopene: (White crystal, M.P. = 35 °C), ^{1}H NMR (200 MHz, $CDCl_3$) δ 7.11 – 7.16 (m, 1H), 7.48 – 7.32 (m, 5H), 7.68 (d, J = 6.0 Hz, 2H).

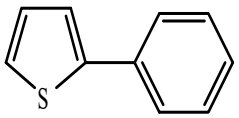

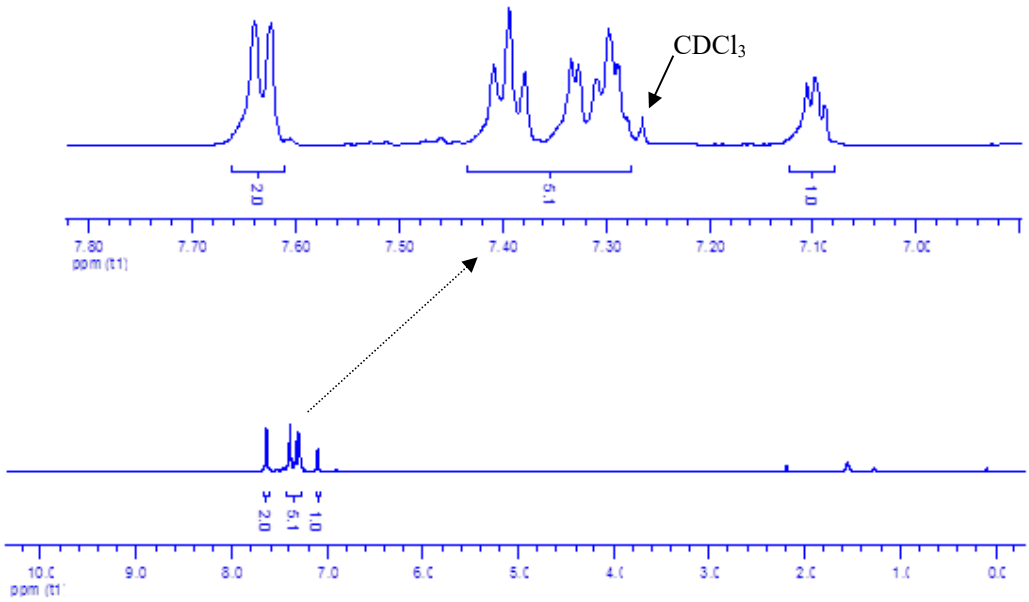

Fig. S45 ^{1}H NMR (200 MHz, $CDCl_3$, 298 K) spectra of 2-phenylthiophene

4-Acetylbiphenyl: (White Solid, M.P. = 121 °C), ^{1}H NMR (300 MHz, $CDCl_3$) δ = 2.65 (s, 3H), 7.40 (t, J = 7.5 Hz, 1H), 7.48 (t, J = 7.5 Hz, 2H), 7.63 (d, J = 9.0 Hz, 2H), 7.69 (d, J = 9.0 Hz, 2H), 8.04 (d, J = 9.0 Hz, 2H).

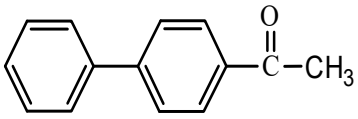

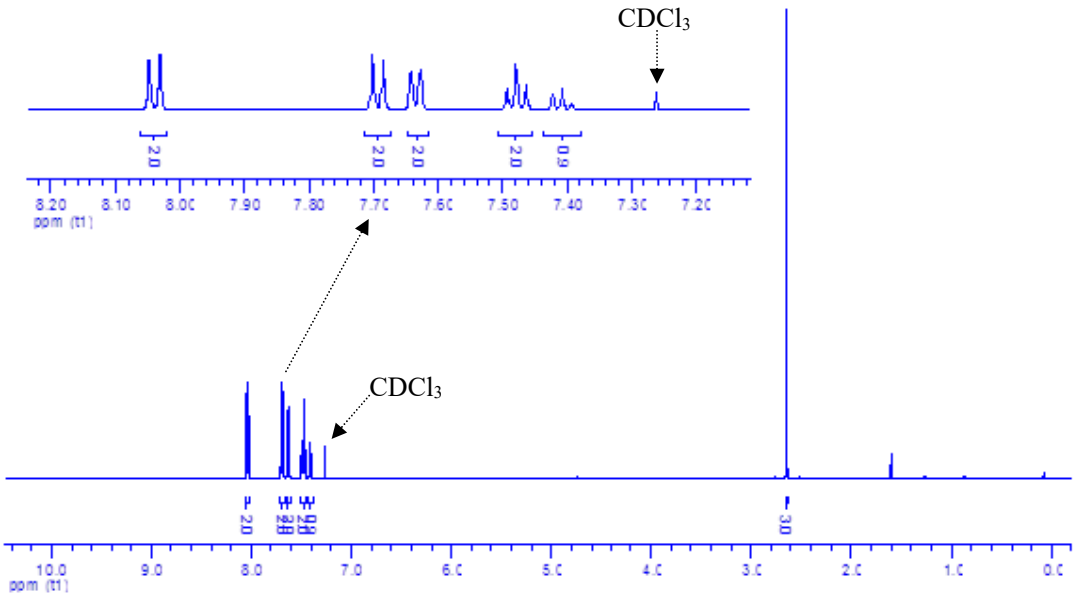

Fig. S46 ^{1}H NMR (300 MHz, $CDCl_3$, 298 K) spectra of 4-acetylbiphenyl

4-Methylbiphenyl: (White solid, M.P. = 49 °C), ^{1}H NMR (500 MHz, $CDCl_3$) δ = 2.41 (s, 3H), 7.26 (d, J = 8.0 Hz, 2H), 7.34 (t, J = 7.2 Hz, 1H), 7.44 (t, J = 7.7 Hz, 2H), 7.51 (d, J = 7.5 Hz, 2H), 7.59 (t, J = 8 Hz, 2H).

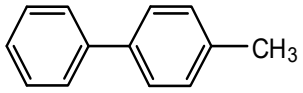

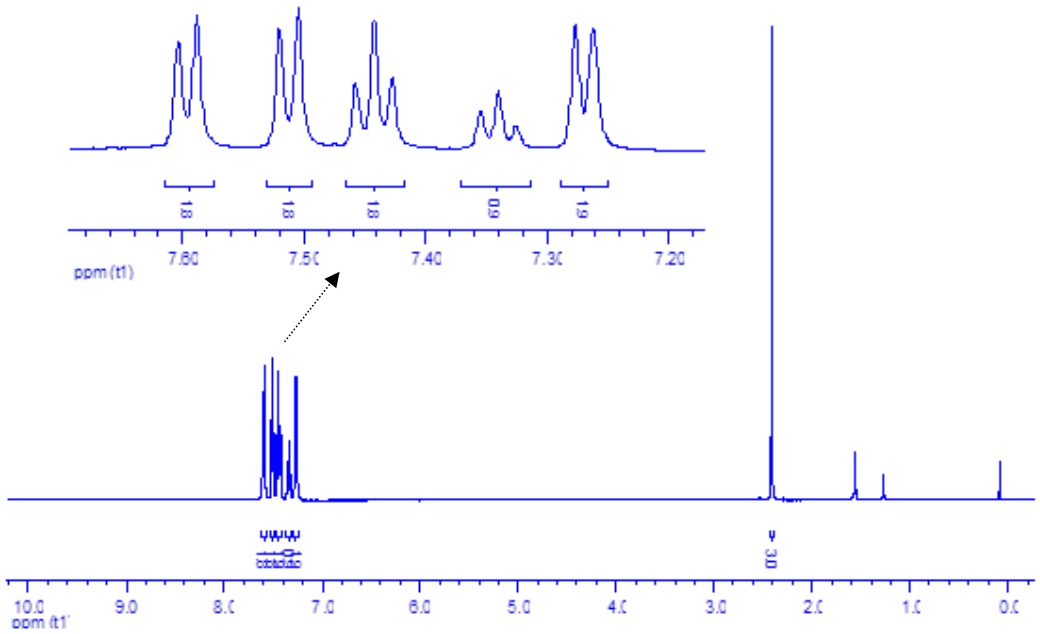

Fig. S47 ^{1}H NMR (500 MHz, CDCl3, 298 K) spectra of 4-methylbiphenyl

4-Nitrobiphenyl: (White-Yellow solid, M.P. = 114 °C), ^{1}H NMR (200 MHz, $CDCl_3$) 7.51 – 7.48 (m, 3H), 7.63 (d, J = 6.0 Hz, 2H), 7.74 (d, J = 10.0 Hz, 1H), 8.30 (d, J = 10.0 Hz, 2H).

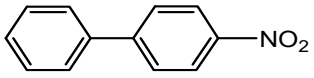

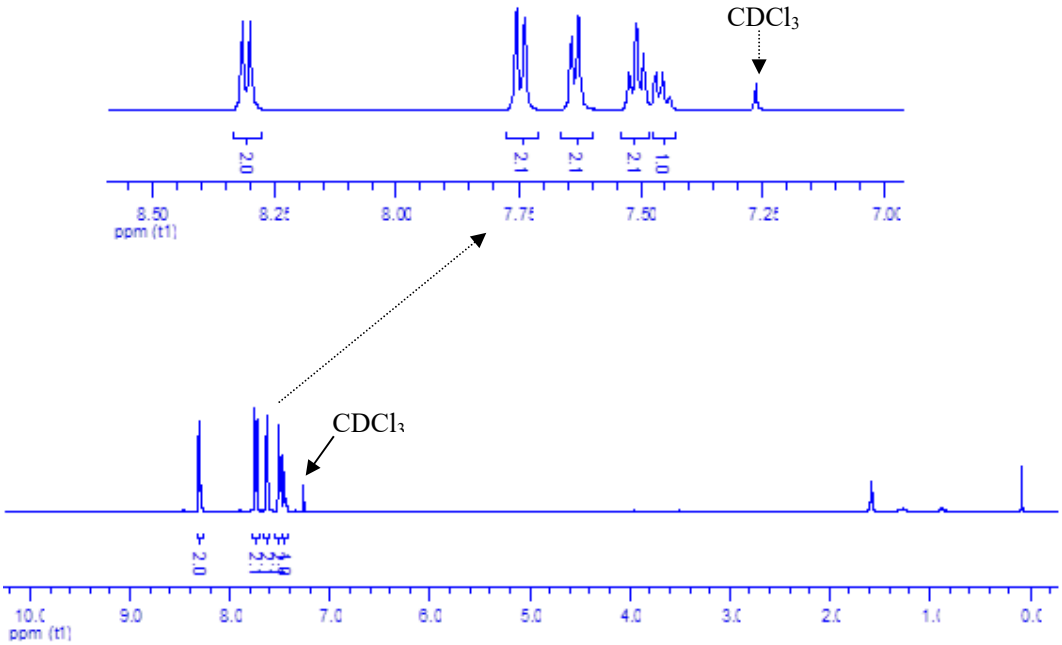

Fig. S48 ^{1}H NMR (200 MHz, CDCl3, 298 K) spectra of 4-nitrobiphenyl

Biphenyl-4-carboxaldehyde: (White-Yellow solid, M.P. = 59 °C), ^{1}H NMR (500 MHz, $CDCl_3$) δ 7.42 (t, J = 7.5 Hz, 1H), 7.49 (t, J = 7.5 Hz, 2H), 7.64 (d, J = 7.0 Hz, 2H), 7.76 (d, J = 8.5 Hz, 2H), 7.96 (d, J = 8.5 Hz, 2H), 10.06 (s, 1H).

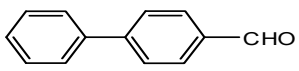

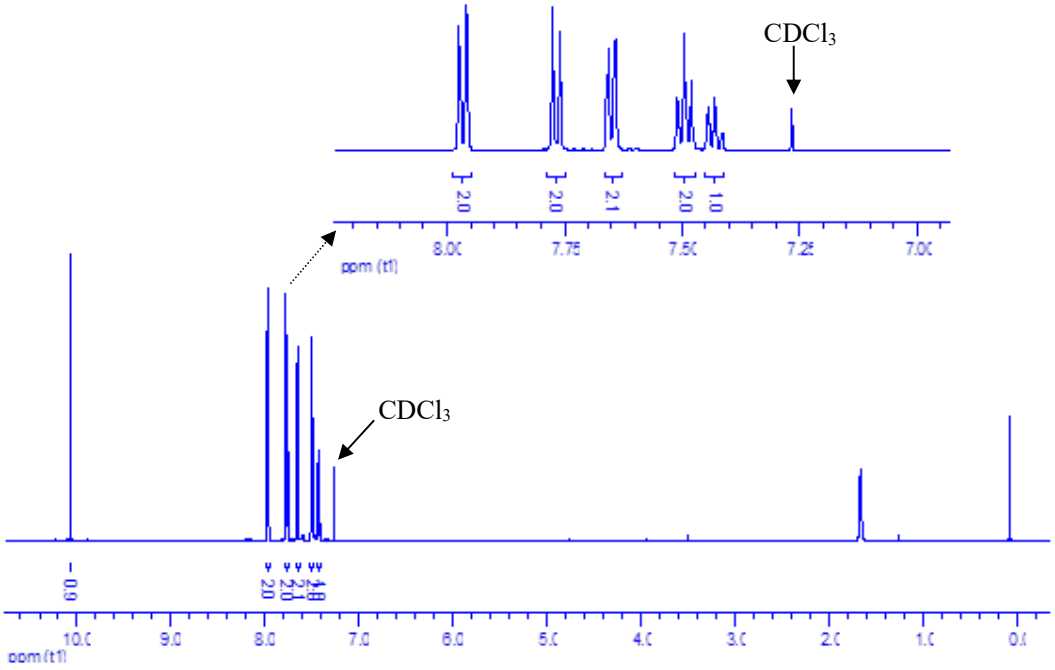

Fig. S49 ^{1}H NMR (500 MHz, $CDCl_3$, 298 K) spectra of biphenyl-4-carbaldehyde

4-Cyanobiphenyl: (White solid, M.P. = 86 °C), ^{1}H NMR (500 MHz, $CDCl_3$) δ 7.43(t, J = 7.5 Hz, 1H), 7.49 (t, J = 5.0 Hz, 2H), 7.59 (d, J = 5.0 Hz, 2H), 7.69 (d, J = 10.0 Hz, 2H), 7.73 (d, J = 10.0 Hz, 2H).

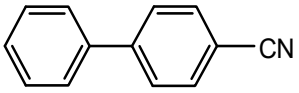

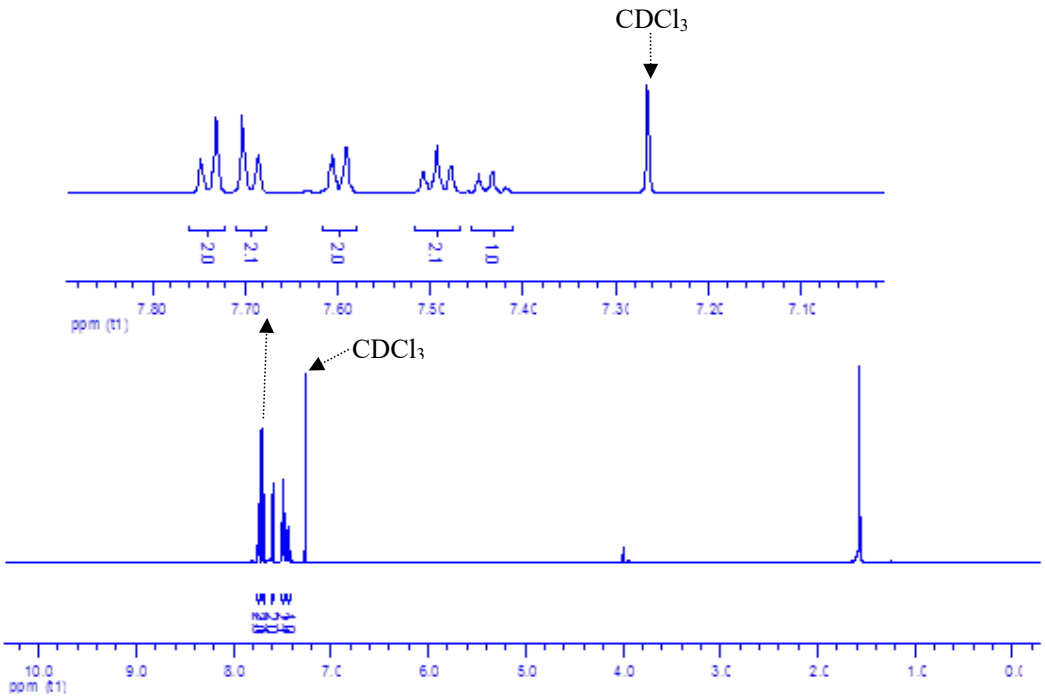

Fig. S50 ^{1}H NMR (500 MHz, $CDCl_3$, 298 K) spectra of 4-cyanobiphenyl**.**

4-Methoxy biphenyl: (White solid, M.P. = 87 °C), ^{1}H NMR (300 MHz, $CDCl_3$) δ 3.86 (s, 3H, CH_3), 6.69-7.00 (m, 2H), 7.27-7.45 (m, 3H), 7.46-7.61 (m, 4H)

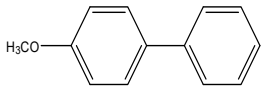

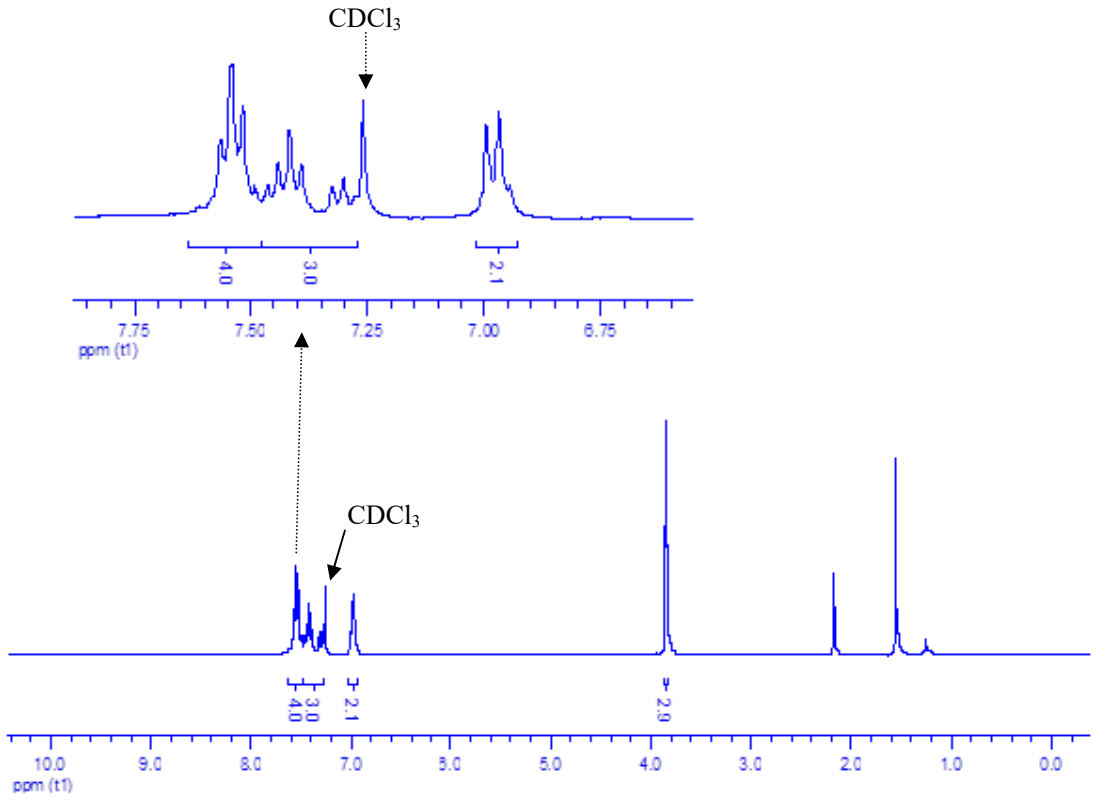

Fig. S51. ^{1}H NMR (300 MHz, $CDCl_3$, 298 K) spectra of 4-methoxy biphenyl.

4-Phenylquinoline: (Oil product), ^{1}H NMR (600 MHz, $CDCl_3$) δ 7.34 (d, J = 3.0 Hz, 1H), 7.51 (m, 6H), 7.73 (t, J = 7.5 Hz, 1H), 7.92 (d, J = 8.4 Hz, 1H), 8.18 (d, J = 8.4 Hz, 1H), 8.94 (d, J = 4.2 Hz, 1H).

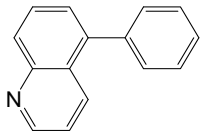

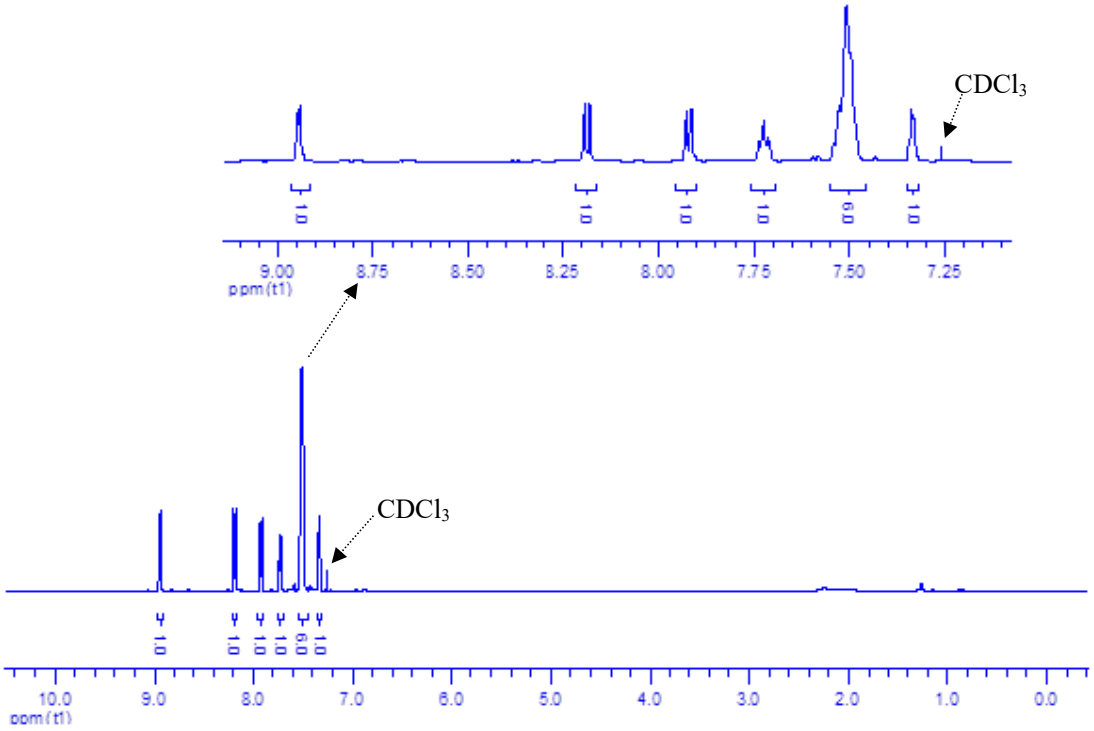

Fig. S52. ^{1}H NMR (600 MHz, $CDCl_3$, 298 K) spectra of 4-phenylquinoline.

1-Phenylnaphthalene: ^{1}H NMR (300 MHz, $CDCl_3$) δ 7.49-7.63 (m, 9H), 7.90-8.05 (m, 3H)

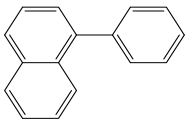

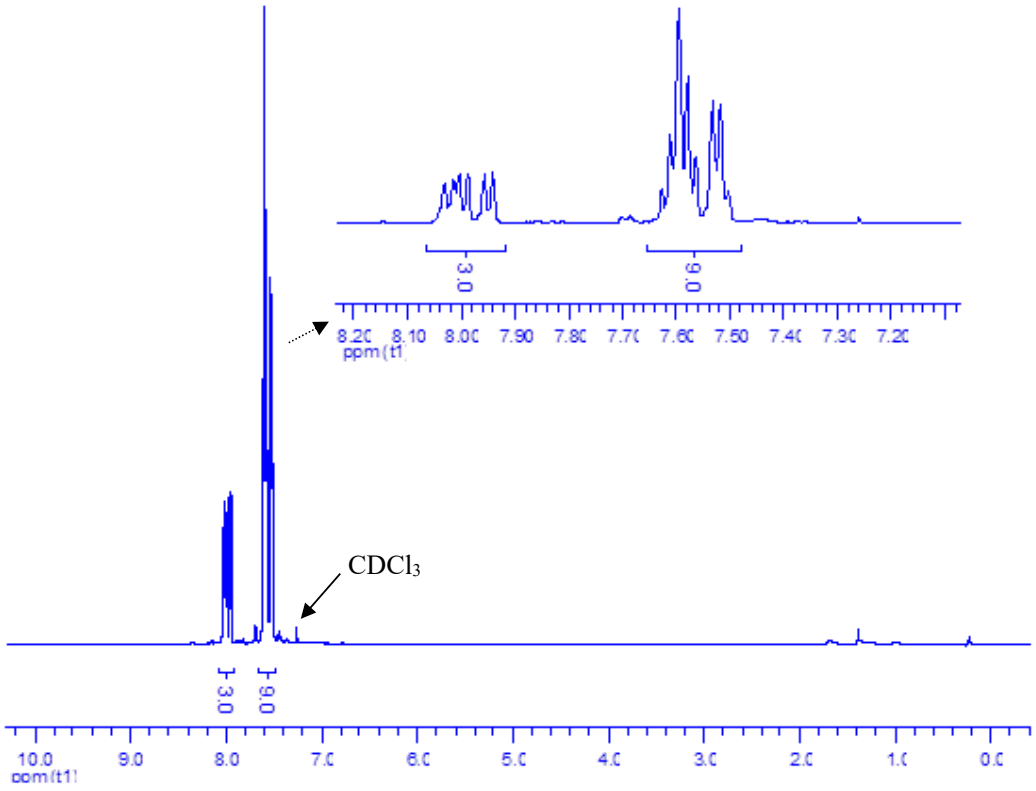

Fig. S53. ^{1}H NMR (300 MHz, $CDCl_3$, 298 K) spectra of 1-phenylnaphthalene.